Supporting Information

Triazolyl-phosphole and triazolyl-azaphosphole: Synthesis, Transition Metal Complexes and Catalytic Studies

Latchupatula Radhakrishna, Basvaraj S. Kote, Rani Gourkhede, Ankit Pandey, Bhupinder Kaur and Maravanji S. Balakrishna*

Phosphorus Laboratory, Department of Chemistry, Indian Institute of Technology Bombay, Powai, Mumbai 400076, India.

*Author to whom correspondence should be addressed. E-mail: krishna@chem.iitb.ac.in, msb_krishna@iitb.ac.in (M. S. Balakrishna); Fax: +91-22-5172-3480/2576-7152

Table of Content

		Page No
1	Crystallographic information for compounds **L1**, **L2**, **1**, **2**, **3**, **5**, and **7**	S3-S5
2	Molecular structures of **3** and **5**	S5-S7
3	NMR spectral data for catalytic products	S7-S9
4	NMR, HRMS and FT-IR spectra of compounds **L1**, **L2**, **$L1_o$**, **$L2_o$** and **1-7**	S10-S33
5	Controlled Experiment	S33-S36
6	NMR spectra of catalytic products	S37-S48
7	References	S49

Crystallographic information for compounds L1, L2, 1, 2, 3, 5, and 7

Table S1. Crystallographic data for compounds L1, L2, and 1.

	L1	**L2**	**1**
Formula	$C_{20}H_{14}N_3P$	$C_{20}H_{14}N_3P$	$C_{31}H_{30}Cl_4N_3PRu$
Formula weight	327.31	327.31	718.42
Temperature/K	150	150	150.15
Crystal system	Triclinic	Monoclinic	Triclinic
Space group	P-1	$P2_1/c$	P-1
a/Å	9.1297(3)	11.9213(8)	9.3109(7)
b/Å	9.3832(4)	8.1536(6)	10.3812(8)
c/Å	11.0431(4)	16.1780(11)	16.2248(10)
α/°	112.436(4)	90	88.026(6)
β/°	95.007(3)	91.743(6)	82.589(6)
γ/°	109.940(4)	90	77.993(6)
Volume/$Å^3$	795.83(6)	1571.80(19)	1521.09(19)
Z	2	4	2
$\rho_{calc}g/cm^3$	1.366	1.383	1.569
F(000)	340	680	728
crystal size, mm^3	0.18×0.12×0.085	0.123×0.076×0.021	0.141×0.021×0.012
μ (MoKα), mm^{-1}	0.178	0.180	0.946
2θ range, deg	4.122 to 62.256	5.038 to 62.444	4.012 to 71.62
Total no. reflns	21476	22157	58324
No.of indep reflns	4719	4757	11099
S	1.051	1.026	1.051
R_1	0.0535	0.0767	0.0623
wR_2	0.1227	0.1658	0.1297

Table S2. **Crystallographic data for complexes 2**, **3, 5 and 7.**

	2	**3**	**5**	**7**
Formula	$C_{30}H_{28}Cl_2N_3PRu$	$C_{40}H_{28}N_6P_2Cl_2Pd$	$C_{25}H_{18}Cl_3N_3PPd$	$C_{40}H_{30}N_6Au_2P_2Cl_2$
Formula weight	633.49	831.92	604.14	1121.47
Temperature/K	150	150.00(10)	100.00(10)	293(2)
Crystal system	Triclinic	Triclinic	triclinic	Monoclinic
Space group	P-1	P-1	P-1	C2
a/Å	10.2927(8)	9.6508(5)	8.33190(10)	17.1377(3)
b/Å	13.3095(13)	11.5561(5)	11.7527(2)	15.0169(2)
c/Å	13.9289(10)	16.7565(8)	13.4917(2)	15.2437(3)
α/°	68.908(8)	79.867(4)	97.1240(10)	90
β/°	78.503(6)	81.712(4)	98.6400(10)	109.761(2)
γ/°	69.443(8)	71.704(4)	110.6210(10)	90
Volume/$Å^3$	1661.1(3)	1738.71(15)	1199.91(3)	3692.02(12)
Z	2	2	2	4
$\rho_{calc}g/cm^3$	1.267	1.589	1.672	2.018
F(000)	644.0	840.0	602.0	2136.0
crystal size, mm	0.132×0.123×0.0042	0.19×0.17×0.057	0.17×0.16×0.063	0.21×0.17×0.057
μ (MoKα), mm^{-1}	0.702	0.820	1.194	8.209
2θ range, deg	3.144 to 72.454	3.748 to 71.422	3.11 to 61.442	3.706 to 62.4
Total no. reflns	61031	88367	9231	56096
No.of indep reflns	11955	13002	5351	11094
S	1.075	1.036	1.187	1.047
R_1	0.1634	0.0935	0.0365	0.0590
wR_2	0.3606	0.1904	0.1033	0.1536

***** The single-crystal X-ray diffraction data for complexes **2**, **3**, **5**, and **7** does not meet the standards required for publication. However, the structures were confirmed without any

ambiguity by spectroscopic and X-ray data. Structures of complexes 2,3,5 and 7 are described in the supporting information.

Molecular structures of *trans*-[(PdCl$_2$){L1-κ^1-*P*}$_2$] (3) and [{Pd(η^3-C$_3$H$_5$)Cl}{{C$_6$H$_5$(1,2,3-N$_3$CC$_6$H$_4$C(PPh)}-κ^1-*P*}] (5)

The perspective view of the molecular structures of complexes **3** and **5** is shown in Fig. 3; the selected bond lengths and angles are listed in figure captions in Fig. 3. The metal center in these complexes adopts slightly distorted square planar geometry. The Pd–P and Pd–Cl bond distances of 2.303(3) and 2.283(3) Å in **3** are similar to those in complexes [PdCl$_2${(DippNH-PPh$_2$)$_2$}-κ^1-P][1] and *trans*-[PdCl$_2$(PPh$_3$)$_2$].[2] The molecular structure of **5** shows a C−H···π interaction between the aromatic proton of one of the phenyl rings and the *ipso* carbon of the PPh moiety (H14···C14 2.816 Å). In addition, complex **5** also displays a C−H···M interaction (H20···Pd1 3.270 Å) between the sp^2 hydrogen of the phenyl sidearm of triazole and the palladium center.

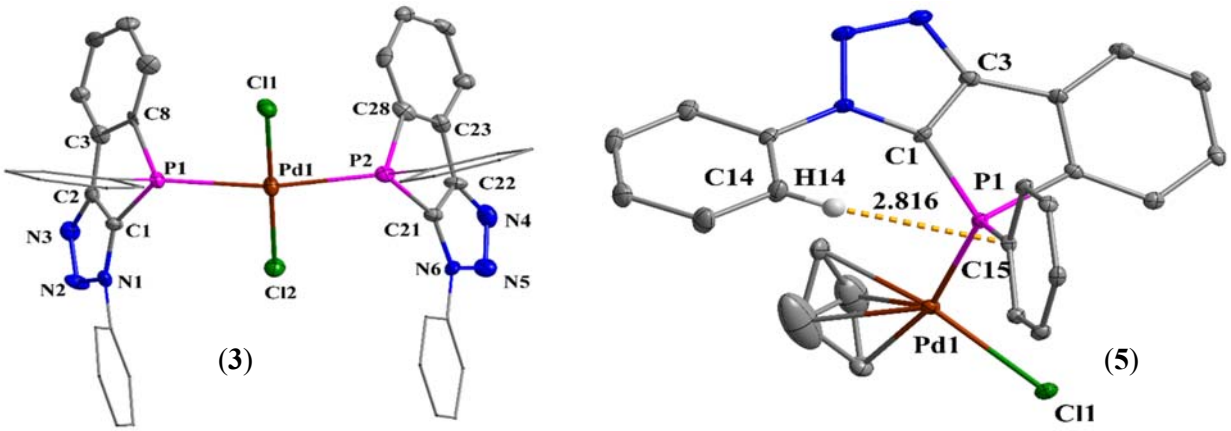

Fig. S1 The molecular structures of *trans*-[(PdCl$_2$)(**L1**-κ^1-*P*)$_2$] (**3**)and [{Pd(η^3 C$_3$H$_5$)Cl}{L2-κ^1-*P*}] (**5**). All hydrogen atoms are omitted for clarity. Displacement ellipsoids are drawn at the 50% probability level. Selected bond lengths (Å) and bond angles (°): For complex **3**: C1–P1 1.793(9), C8–P1 1.840(10), P1–Pd1 2.298(3), P2–Pd1 2.303(3), Pd1–Cl1 2.312(3), Pd2–Cl2 2.283(3), C1–P1–Pd1 119.0(4), P1–Pd1–P2 166.88(10), Cl1–Pd1–Cl2 176.37(11). For

complex **5**: C1–P1 1.810(4), C15–P1 1.817(4), C8–P1 1.834(4), P1–Pd1 2.2780(11), Pd1–Cl1 2.3869(11), C1–P1–C15 105.0(2), C1–P1–Pd1 118.92(14), P1–Pd1–Cl1 96.58(4).

Molecular structure of [(AuCl){L1-κ^1-*P*}] (7)

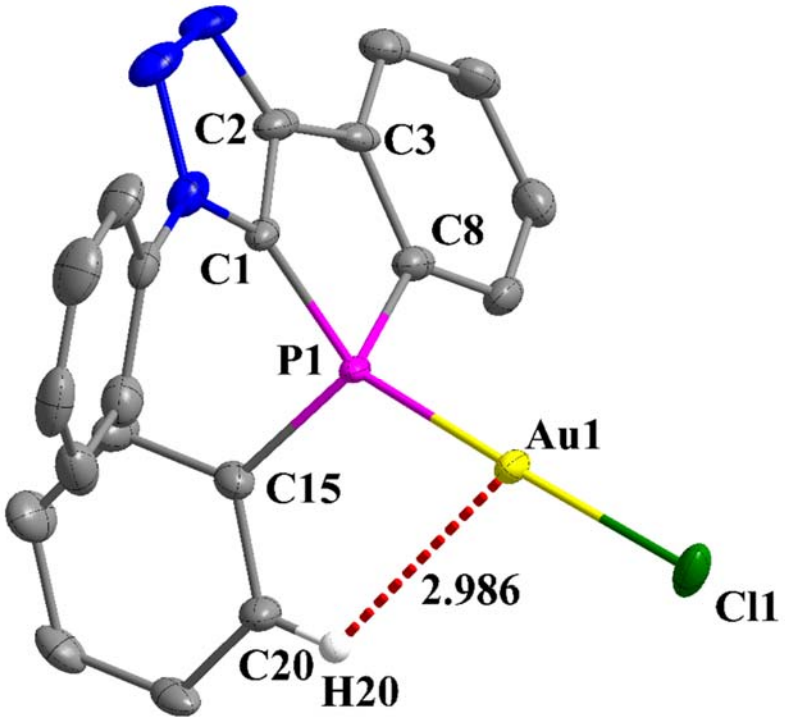

Fig. S2 The molecular structure of [(AuCl){L1-κ^1-*P*}] (**7**). All hydrogen atoms are omitted for clarity. Selected bond lengths (Å) and bond angles (°): C1–P1 1.790(7), Au1–P1 2.216(2), Au1–Cl1 2.288(2), P1−C15 1.817(8), P1−C8 1.848(8), C1–P1–C15 105.7(4), C1–P1–C8 89.5(4), C15–P1–C8 106.5(4), Cl1–Au1–P1 171.16(8).

The crystals of **7** suitable for single-crystal X-ray diffraction study were obtained by crystallizing in 1:1 mixture of chloroform and petroleum ether at room temperature over 36 h. The molecular structure of **7** along with selected bond distances and bond angles is shown in Fig. 4. The Au^I center adopts linear geometry with a bond angle of 178.35(2)° (P1-Au1-Cl1). The Au1–P1 and Au1–Cl1 bond distances 2.2279(5) and 2.2741(6) Å in **7** are in the range

found in analogous complexes.[3] The ortho-hydrogen of phenyl group from PPh moiety is in close proximity to Au atom with a H20···Au1 distance of 2.985 Å.

NMR spectral data of catalytic products of Ru(II) catalysed benzylic oxidation reaction

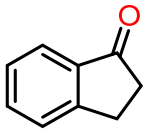

1-indanone *(**1a**)*: Purified by column chromatography on silica gel using petroleum ether and ethyl acetate as eluents, 90 % (118 mg) yield as white solid. ^{1}H NMR (500 MHz, CDCl3): δ 7.76 (d, *J* = 7.7 Hz, 1H), 7.58 (td, *J* = 7.5, 1.2 Hz, 1H), 7.48 (dt, *J* = 7.7, 1.0 Hz, 1H), 7.38 – 7.35 (m, 1H), 3.19 – 3.11 (m, 2H), 2.72 – 2.65 (m, 2H). ^{13}C NMR (126 MHz, $CDCl_3$): δ 207.2, 155.2, 134.6, 128.3, 127.3, 126.7, 123.8, 36.2, 25.8.

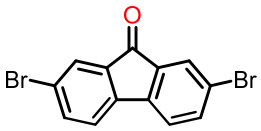

2,7-dibromo-9H-fluoren-9-one *(**1b**)*. Purified by column chromatography on silica gel using petroleum ether and ethyl acetate as eluents, 92 % (310.95 mg) yield as yellow solid. ^{1}H NMR (400 MHz, $CDCl_3$): δ 7.73 (d, *J* = 5.3 Hz, 2H), 7.66 – 7.55 (m, 2H), 7.44 – 7.28 (m, 2H). ^{13}C NMR (101 MHz, $CDCl_3$): δ 191.0, 142.4, 137.6, 135.4, 128.0, 123.5, 122.0.

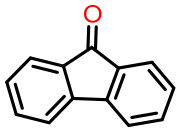

9H-fluoren-9-one *(**1c**)*. Purified by column chromatography on silica gel using petroleum ether and ethyl acetate as eluents, 94 % (169.39 mg) yield as yellow solid. ^{1}H NMR (500 MHz, $CDCl_3$): δ 7.66 – 7.61 (m, 2H), 7.50 – 7.41 (m, 4H), 7.27 (td, *J* = 7.0, 1.8 Hz, 2H). ^{13}C NMR (126 MHz, $CDCl_3$): δ 193.9, 144.4, 134.7, 134.2, 129.1, 124.3, 120.3.

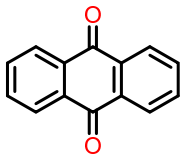

Anthracene-9,10-dione *(**1d**)*. Purified by column chromatography on silica gel using petroleum ether and ethyl acetate as eluents, 88 % (183.23 mg) yield as white solid. ^{1}H NMR (500 MHz, $CDCl_3$): δ 8.32 (dd, *J* = 5.7, 3.3 Hz, 4H), 7.80 (dd, *J* = 5.8, 3.3 Hz,4H). ^{13}C NMR (126 MHz, $CDCl_3$): δ 183.3, 134.3, 133.7, 127.4.

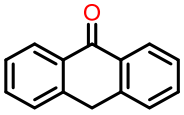

Anthracen-9(10H)-one *(**1e**)*. Purified by column chromatography on silica gel using petroleum ether and ethyl acetate as eluents, 75 % (145.67 mg) yield as white solid. ^{1}H NMR (500 MHz, $CDCl_3$): δ 8.46 – 8.25 (m, 2H), 7.56 (ddd, *J* = 7.6, 5.6, 2.2 Hz, 2H), 7.50 – 7.38 (m, 4H), 4.41 – 4.17 (m, 2H). ^{13}C NMR (126 MHz, $CDCl_3$): δ 184.3, 140.5, 132.8, 132.1, 127.6 (d, *J* = 2.2 Hz), 127.1, 32.3.

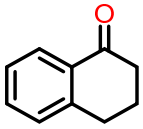

3,4-dihydronaphthalen-1(2H)-one *(**1f**)*. Purified by column chromatography on silica gel using petroleum ether and ethyl acetate as eluents, 94 % (137.41 mg) yield as a colorless liquid. ^{1}H NMR (500 MHz, $CDCl_3$): δ 7.46 (s, 1H), 7.37 – 7.28 (m, 1H), 7.25 (d, *J* = 7.7 Hz, 2H), 2.69 – 2.61 (m, 6H). ^{13}C NMR (126 MHz, $CDCl_3$): δ 198.8, 144.6, 134.8, 132.5, 128.8, 127.2, 126.6, 39.1, 29.7, 23.3.

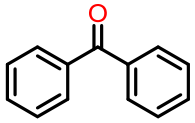

Benzophenone *(**1g**)*. Purified by column chromatography on silica gel using petroleum ether and ethyl acetate as eluents, 99 % (180.39 mg) yield as white solid. ^{1}H NMR (500 MHz, $CDCl_3$): δ 7.81 (dd, *J* = 8.3, 1.4 Hz, 4H), 7.58 (s, 2H), 7.48 (t, *J* = 7.7 Hz, 4H). ^{13}C NMR (126 MHz, $CDCl_3$): δ 196.8, 137.7, 132.5, 130.1, 128.4.

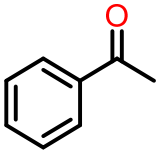

Acetophenone *(**1h**)*. Purified by column chromatography on silica gel using petroleum ether and ethyl acetate as eluents, 61 % (73.29 mg) yield as a colourless liquid. ^{1}H NMR (500 MHz, $CDCl_3$): δ 8.02 – 7.86 (m, 1H), 7.51 (dddq, *J* = 7.1, 4.4, 3.1, 1.5 Hz, 1H), 7.45 – 7.35 (m, 1H), 2.59 – 2.51 (m, 2H). ^{13}C NMR (126 MHz, $CDCl_3$): δ 198.0, 137.1, 133.1, 128.4 (d, *J* = 35.0 Hz), 26.5.

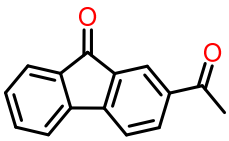

2-acetyl-9H-fluoren-9-one *(**1i**)*. Purified by column chromatography on silica gel using petroleum ether and ethyl acetate as eluents, 95 % (211.12 mg) yield as yellow solid. ^{1}H NMR (500 MHz, $CDCl_3$): δ 8.27 – 8.15 (m, 1H), 8.16 – 8.12 (m, 1H), 7.73 – 7.67 (m, 1H), 7.60 (tdd, *J* = 7.2, 5.7, 2.9 Hz, 2H), 7.56 – 7.50 (m, 1H), 7.37 (ddd, *J* = 10.8, 5.4, 2.6 Hz, 1H), 2.63 (s, 3H). ^{13}C NMR (126 MHz, $CDCl_3$): δ 196.7, 192.8, 148.6, 143.4, 138.0, 135.1 (d, *J* = 17.1 Hz), 134.5, 130.4, 124.8, 124.3, 121.4, 120.6, 26.8.

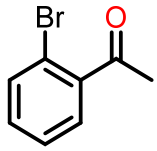

1-(2-bromophenyl)ethan-1-one *(**1l**)*. Purified by column chromatography on silica gel using petroleum ether and ethyl acetate as eluents, 44 % (87.58 mg) yield as a colorless liquid. ^{1}H NMR (400 MHz, $CDCl_3$): δ 7.64 (ddt, *J* = 7.3, 3.5, 1.6 Hz, 1H), 7.31 (dt, *J* = 7.6, 1.9 Hz, 1H), 7.25 – 7.14 (m, 2H), 2.57 – 2.47 (m, 3H). ^{13}C NMR (101 MHz, $CDCl_3$): δ 201.4, 138.3, 137.4, 131.9, 129.3, 125.6, 21.5.

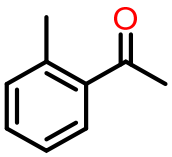

1-(o-tolyl)ethan-1-one *(**1m**)*. Purified by column chromatography on silica gel using petroleum ether and ethyl acetate as eluents, 44 % (59.03 mg) yield as a colourless liquid. ^{1}H NMR (400 MHz, $CDCl_3$): δ 7.68 – 7.60 (m, 1H), 7.32 (s, 1H), 7.25 – 7.14 (m, 2H), 2.52 (s, 3H), 2.49 (s, 3H). ^{13}C NMR (101 MHz, $CDCl_3$): δ 201.4, 138.3, 137.4, 131.9, 131.4, 129.3, 125.6, 29.3, 21.5.

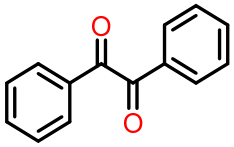

Benzil: *(**1n**)*. Purified by column chromatography on silica gel using petroleum ether and ethyl acetate as eluents, 56 % (117.72 mg) yield as white solid. ^{1}H NMR (400 MHz, $CDCl_3$): δ 7.98 (dd, *J* = 8.3, 1.4 Hz, 3H), 7.71 – 7.62 (m,2H), 7.57 – 7.46 (m,4H). ^{13}C NMR (101 MHz, $CDCl_3$): δ 194.7, 135.0, 133.1, 130.0, 129.2.

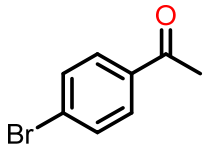

1-(4-bromophenyl)ethan-1-one *(**1o**)*. Purified by column chromatography on silica gel using petroleum ether and ethyl acetate as eluents, 52 % (103.50 mg) yield as a colourless liquid. ^{1}H NMR (500 MHz, $CDCl_3$): δ 8.01 – 7.77 (m, 2H), 7.75 – 7.50 (m, 2H), 2.64 (s, 3H). ^{13}C NMR (126 MHz, $CDCl_3$): δ 197.1, 135.9, 132.0 (d, *J* = 3.0 Hz), 130.0 (d, *J* = 3.3 Hz), 128.4, 26.7.

NMR, HRMS and FT-IR spectra of compounds 1-10

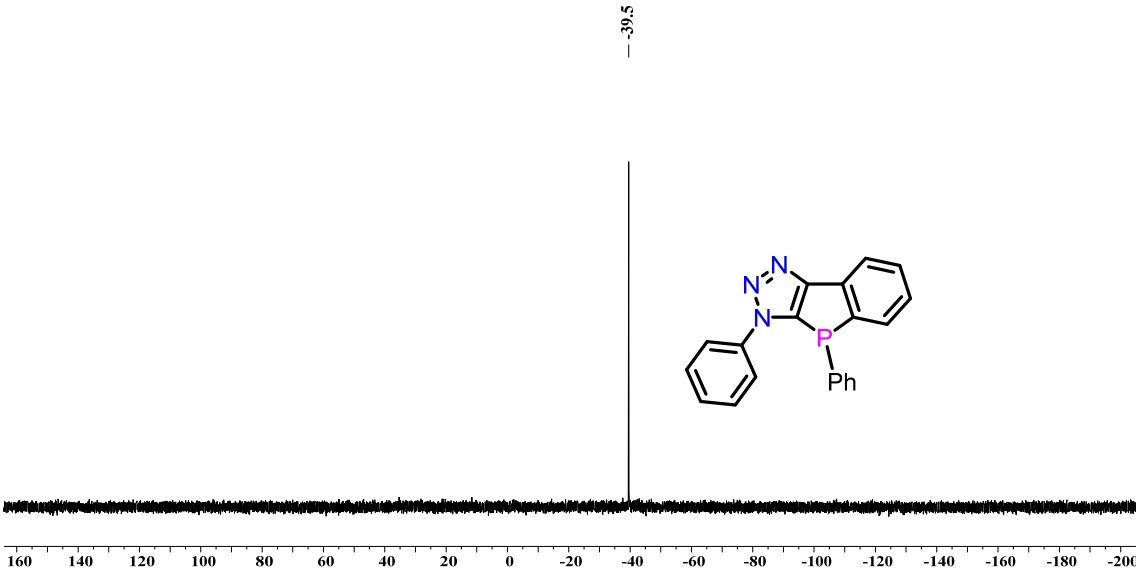

Fig. S3 $^{31}P\{^{1}H\}$ NMR spectrum of **L1** in $CDCl_3$ (162 MHz).

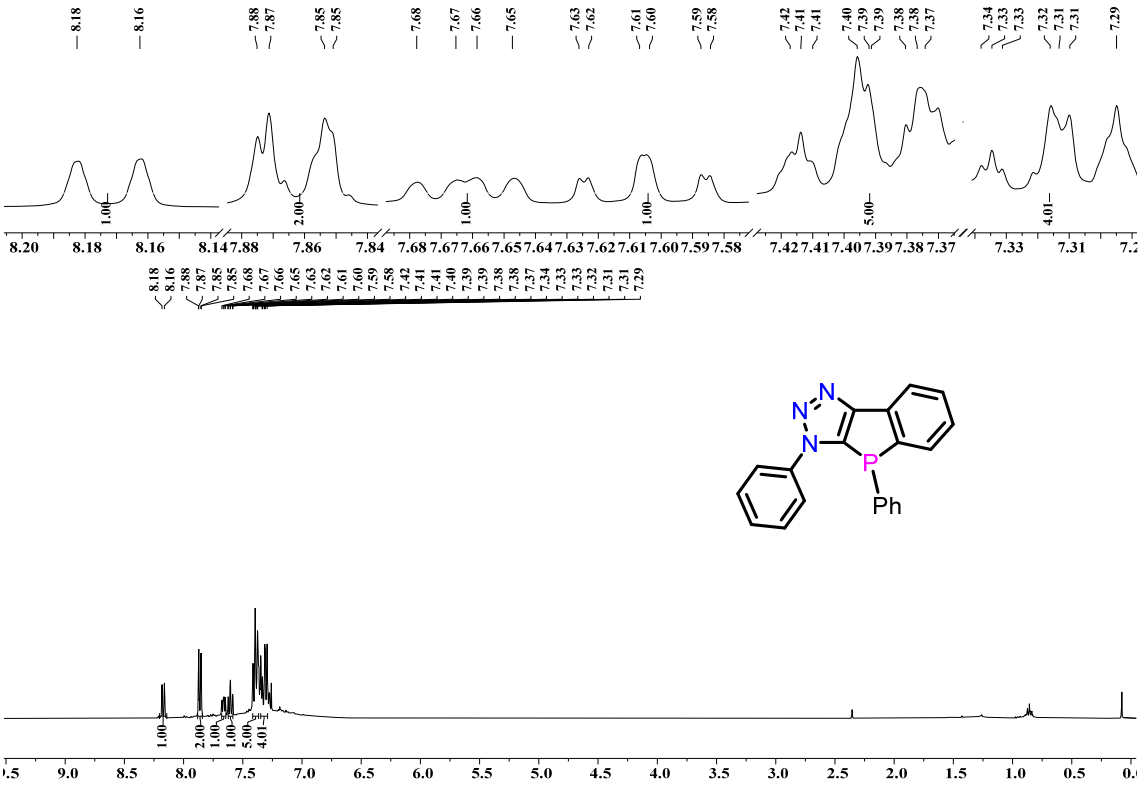

Fig. S4 ^{1}H NMR spectrum of **L1** in $CDCl_3$ (400 MHz).

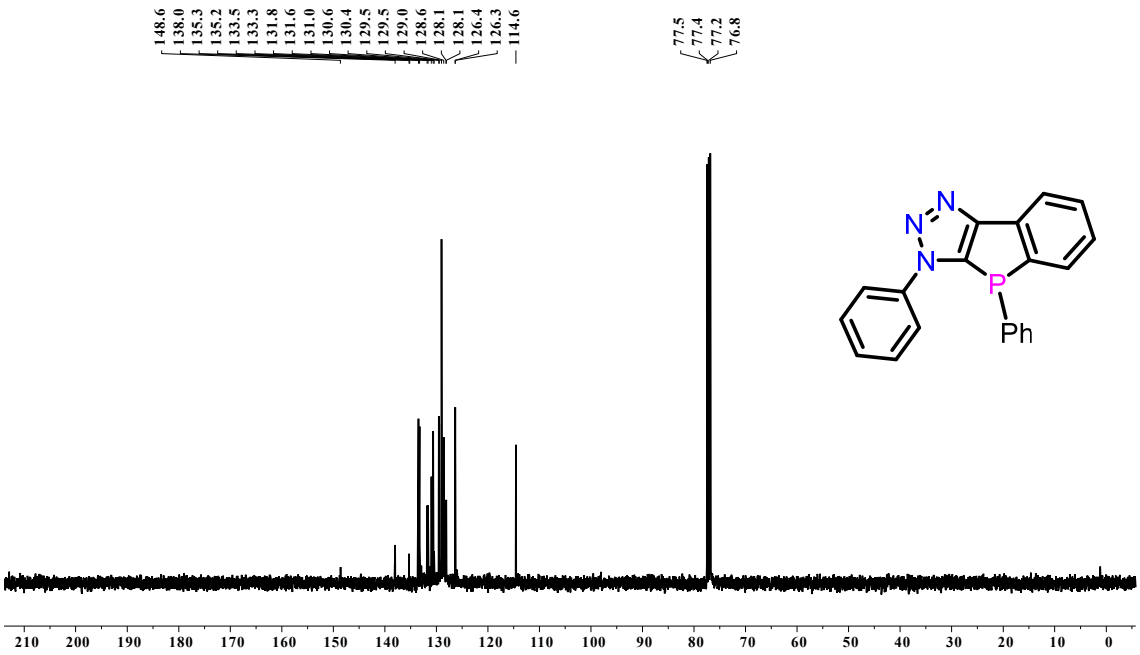

Fig. S5 $^{13}C\{^{1}H\}$ NMR spectrum of **L1** in $CDCl_3$ (101 MHz).

DEPARTMENT OF CHEMISTRY, I.I.T.(B)

Analysis Info

Analysis Name	D:\Data\OCT-2021\MSB-BK-PHOSPHOLE-A.d	Acquisition Date	10/30/2021 11:29:34 PM
Method	Low_mass- NaICsI.m	Operator	PPI IN
Sample Name	MSB-BK-PHOSPHOLE-A	Instrument	maXis impact 282001.00081
Comment	C20H14N3P1		

Acquisition Parameter

Source Type	ESI	Ion Polarity	Positive	Set Nebulizer	0.3 Bar
Focus	Not active	Set Capillary	4000 V	Set Dry Heater	180 °C
Scan Begin	50 m/z	Set End Plate Offset	-500 V	Set Dry Gas	4.0 l/min
Scan End	650 m/z	Set Charging Voltage	2000 V	Set Divert Valve	Source
		Set Corona	0 nA	Set APCI Heater	0 °C

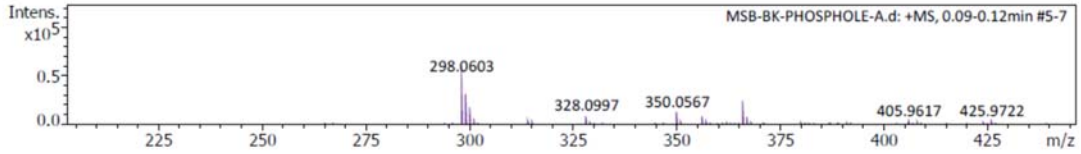

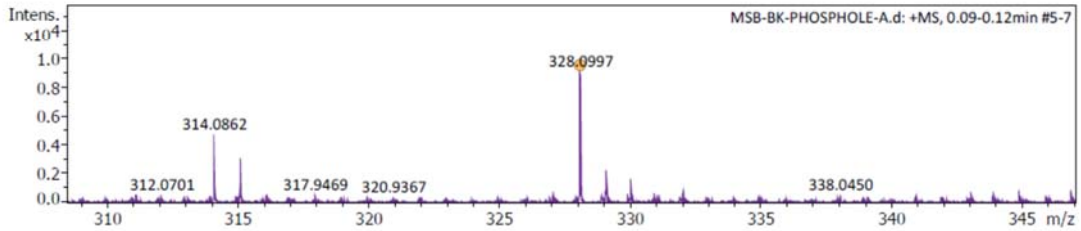

Meas. m/z	#	Ion Formula	m/z	err [ppm]	mSigma	# mSigma	Score	rdb	e⁻ Conf	N-Rule
328.0997	1	C20H15N3P	328.0998	0.2	15.9	1	100.00	17.0	even	ok

Fig. S6 HRMS spectrum of **L1**.

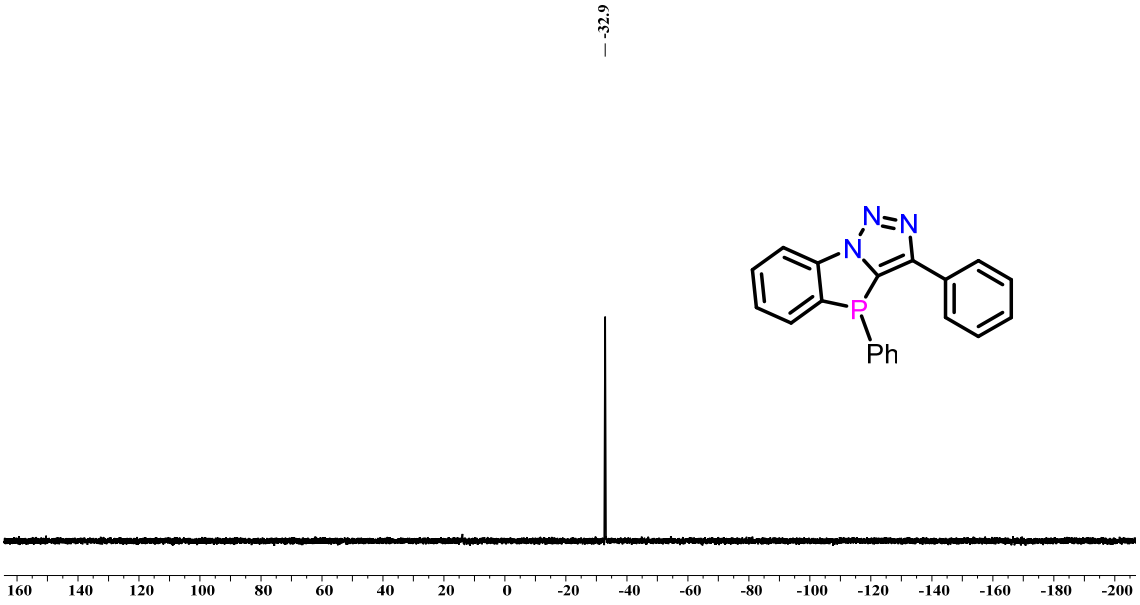

Fig. S7 $^{31}P\{^{1}H\}$ NMR spectrum of **L2** in $CDCl_3$ (162 MHz).

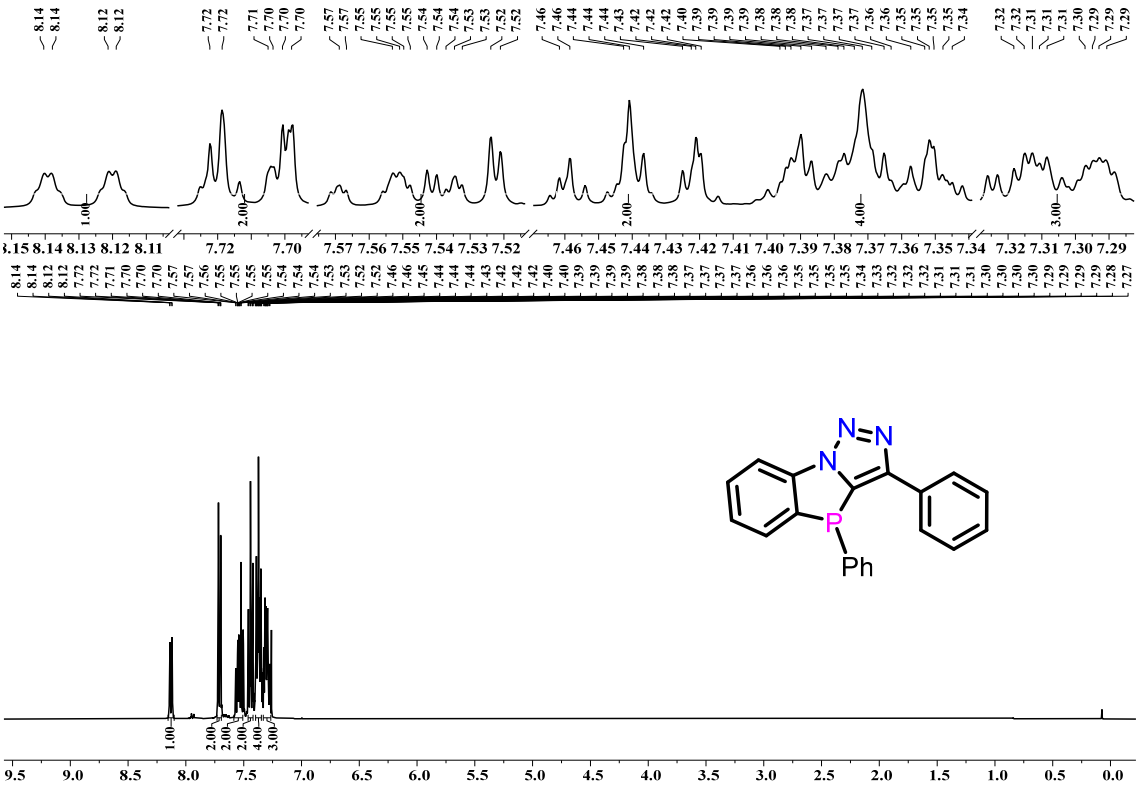

Fig. S8 ^{1}H NMR spectrum of **L2** in $CDCl_3$ (400 MHz).

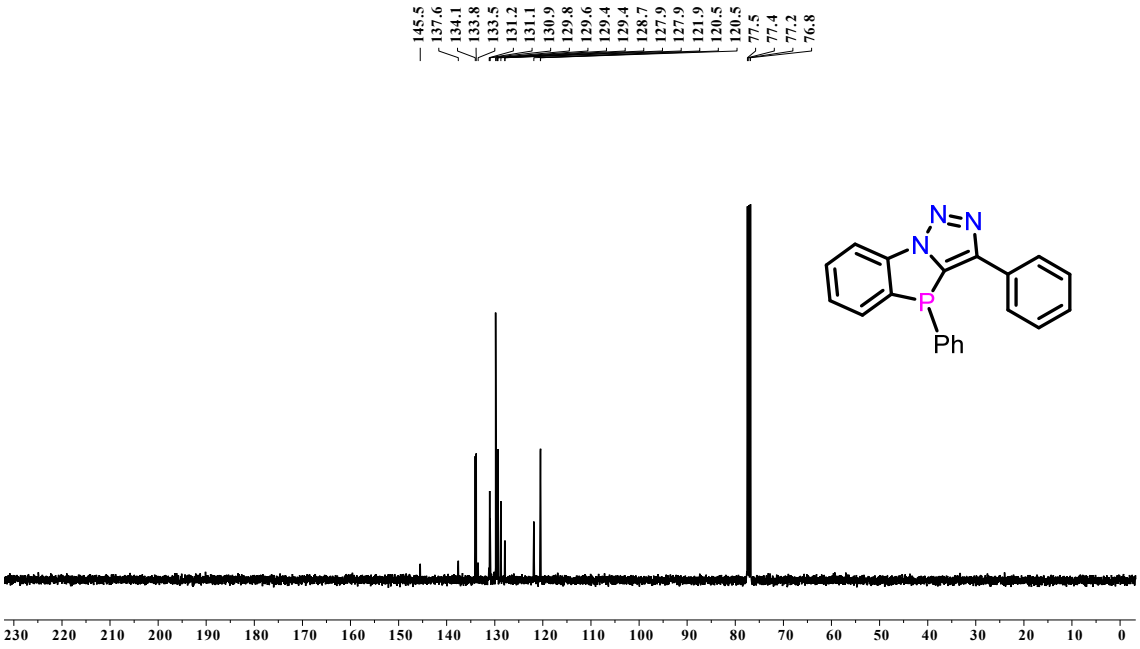

Fig. S9 $^{13}C\{^{1}H\}$ NMR spectrum of **L2** in $CDCl_3$ (101 MHz).

DEPARTMENT OF CHEMISTRY, I.I.T.(B)

Analysis Info

Analysis Name	D:\Data\OCT-2021\MSB-BK-AZAPHOSPHOLE.d	Acquisition Date	10/30/2021 11:30:12 PM
Method	Low_mass- NaICsI.m	Operator	PPI IN
Sample Name	MSB-BK-AZAPHOSPHOLE	Instrument	maXis impact 282001.00081
Comment	C20H14N3P1		

Acquisition Parameter

Source Type	ESI	Ion Polarity	Positive	Set Nebulizer	0.3 Bar
Focus	Not active	Set Capillary	4000 V	Set Dry Heater	180 °C
Scan Begin	50 m/z	Set End Plate Offset	-500 V	Set Dry Gas	4.0 l/min
Scan End	650 m/z	Set Charging Voltage	2000 V	Set Divert Valve	Source
		Set Corona	0 nA	Set APCI Heater	0 °C

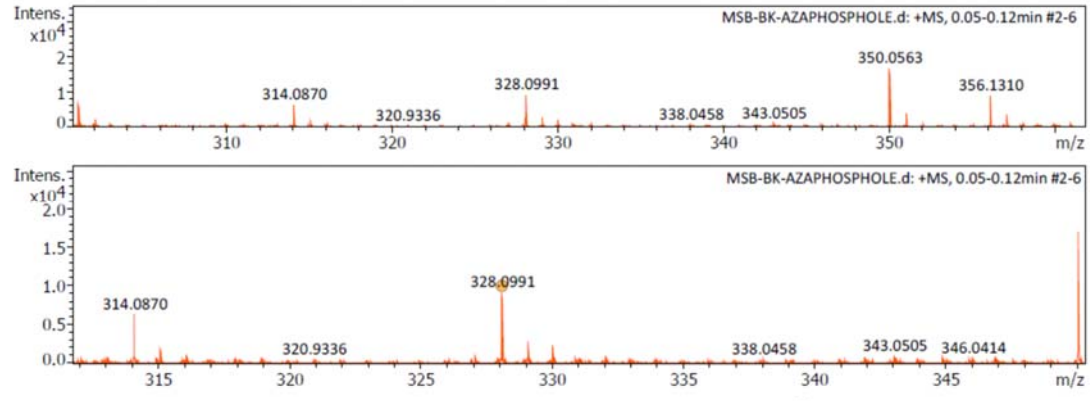

Meas. m/z	#	Ion Formula	m/z	err [ppm]	mSigma	# mSigma	Score	rdb	e⁻ Conf	N-Rule
328.0991	1	C20H15N3P	328.0998	2.2	50.9	1	100.00	17.0	even	ok

Fig. S10 HRMS spectrum of **L2**.

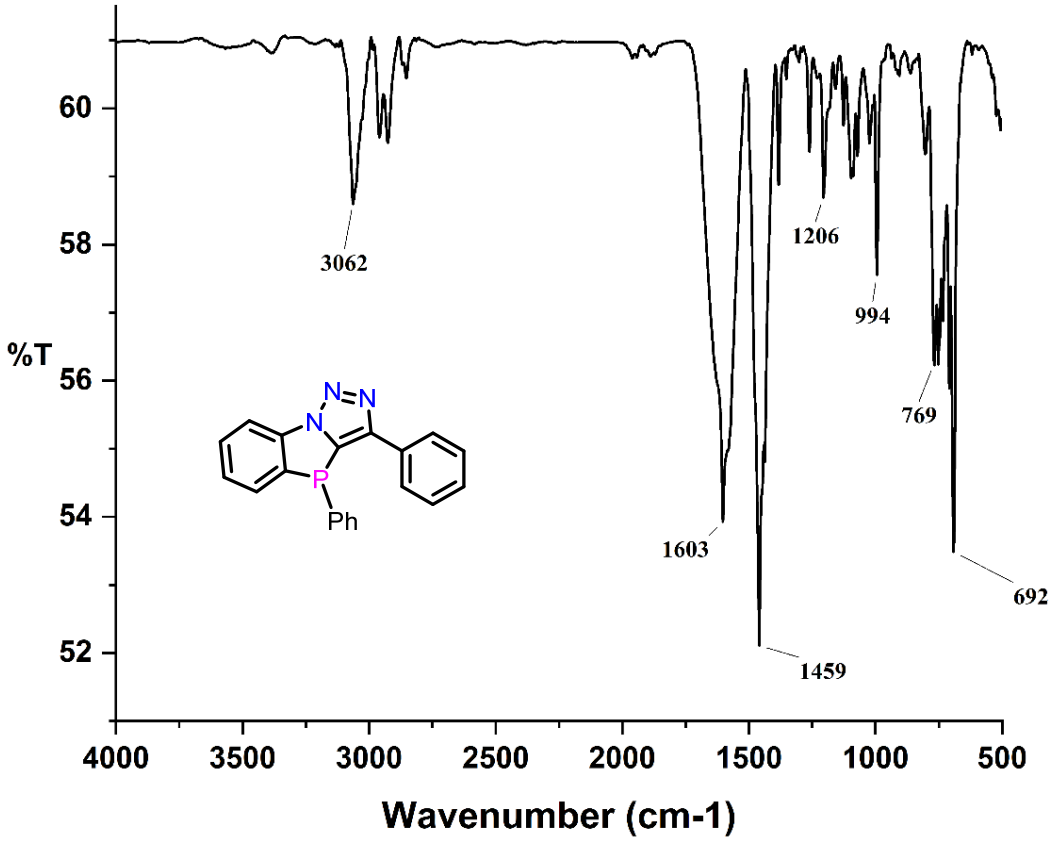

Fig. S11 FT-IR spectrum of compound **L2**.

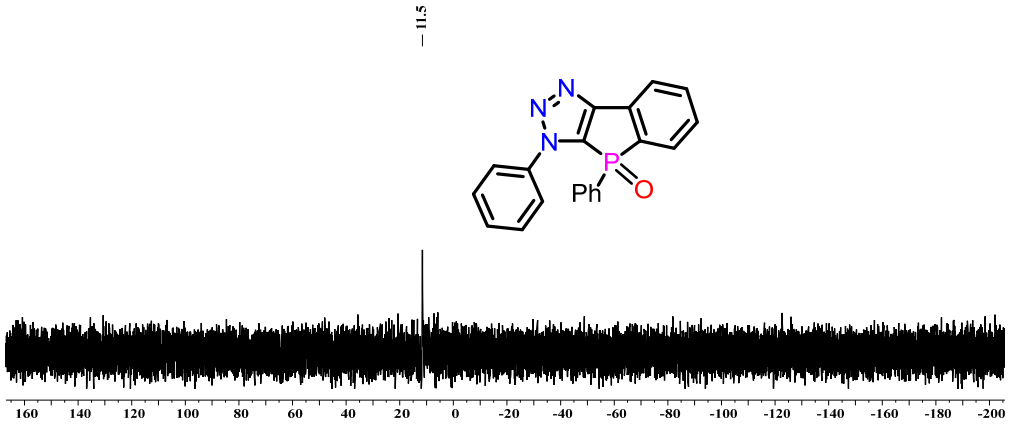

Fig. S12 $^{31}P\{^{1}H\}$ NMR spectrum of **L1o** in $CDCl_3$ (162 MHz).

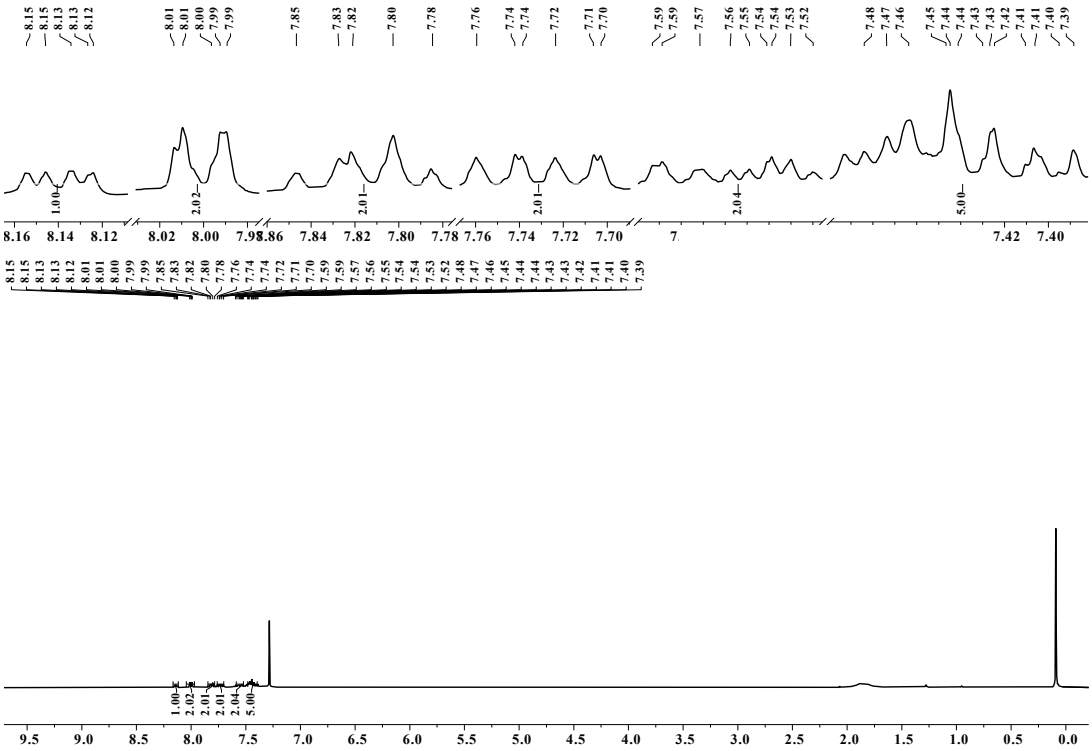

Fig. S13 ^{1}H NMR spectrum of **L1O** in $CDCl_3$ (400 MHz).

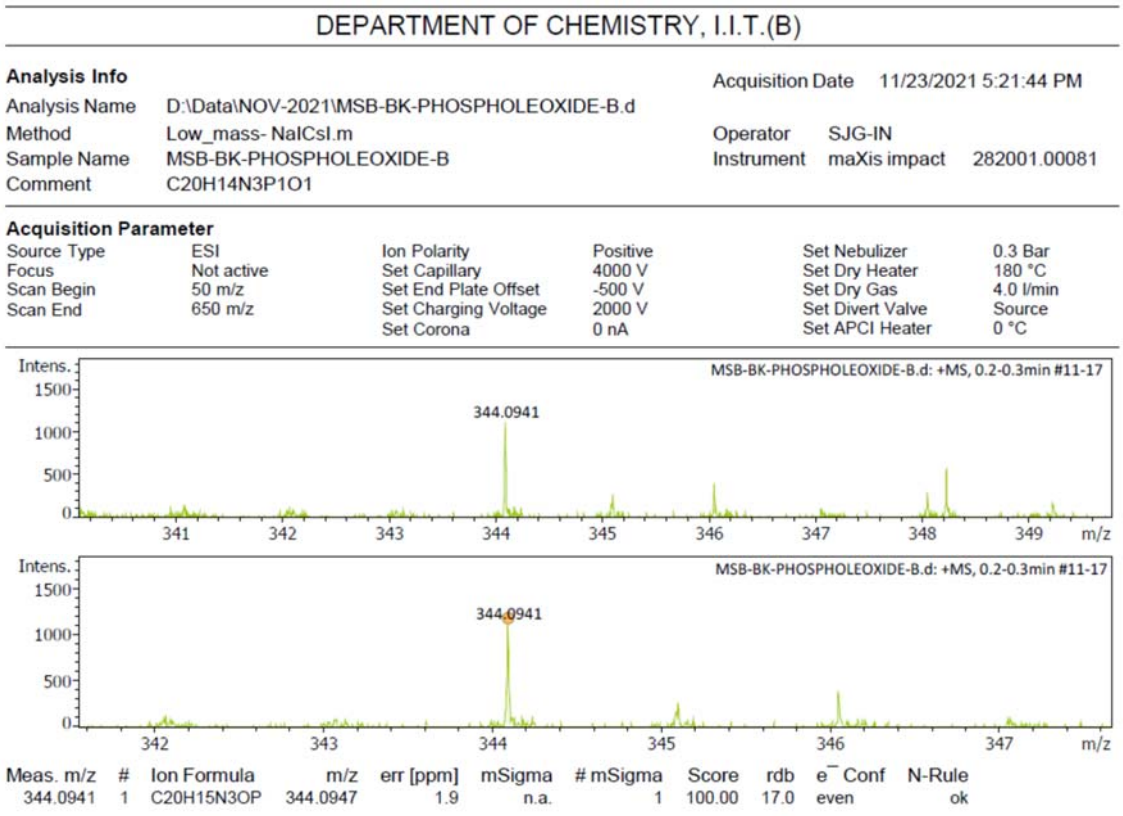

DEPARTMENT OF CHEMISTRY, I.I.T.(B)

Analysis Info

Analysis Name	D:\Data\NOV-2021\MSB-BK-PHOSPHOLEOXIDE-B.d	Acquisition Date	11/23/2021 5:21:44 PM
Method	Low_mass- NaICsI.m	Operator	SJG-IN
Sample Name	MSB-BK-PHOSPHOLEOXIDE-B	Instrument	maXis impact 282001.00081
Comment	C20H14N3P1O1		

Acquisition Parameter

Source Type	ESI	Ion Polarity	Positive	Set Nebulizer	0.3 Bar
Focus	Not active	Set Capillary	4000 V	Set Dry Heater	180 °C
Scan Begin	50 m/z	Set End Plate Offset	-500 V	Set Dry Gas	4.0 l/min
Scan End	650 m/z	Set Charging Voltage	2000 V	Set Divert Valve	Source
		Set Corona	0 nA	Set APCI Heater	0 °C

Meas. m/z	#	Ion Formula	m/z	err [ppm]	mSigma	# mSigma	Score	rdb	e¯ Conf	N-Rule
344.0941	1	C20H15N3OP	344.0947	1.9	n.a.	1	100.00	17.0	even	ok

Fig. S14 HRMS spectrum of **L1O**.

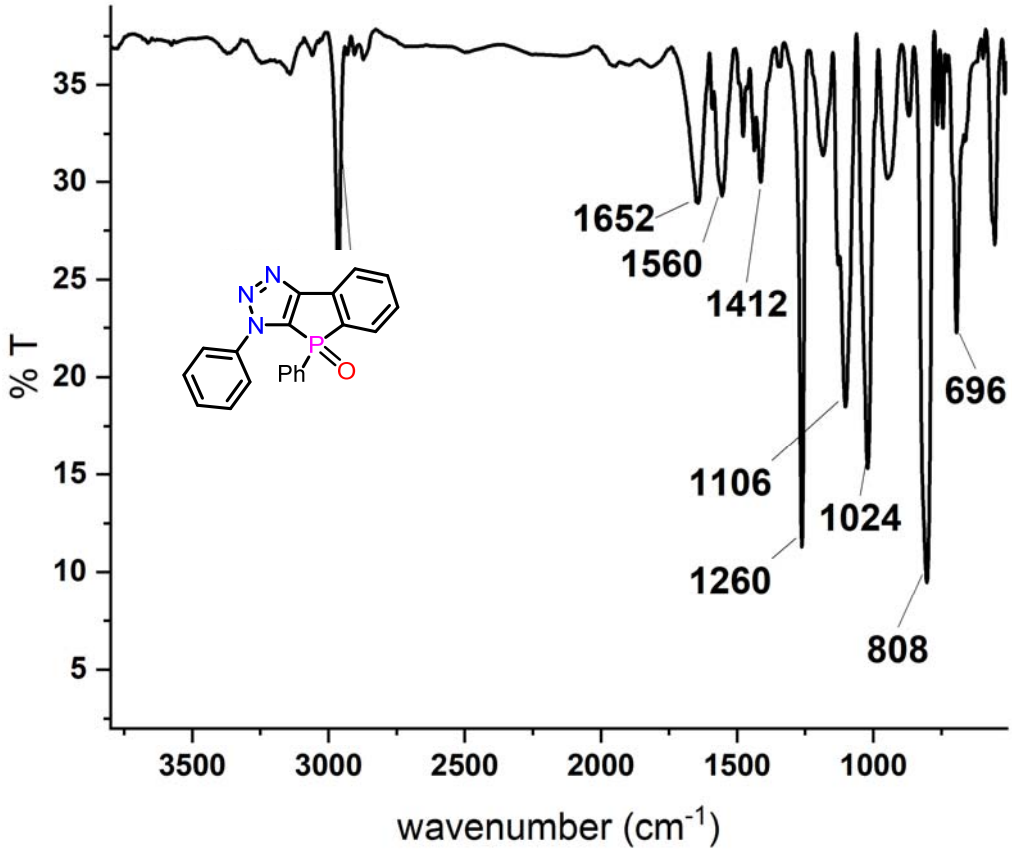

Fig. S15 FT-IR spectrum of compound **L1o**.

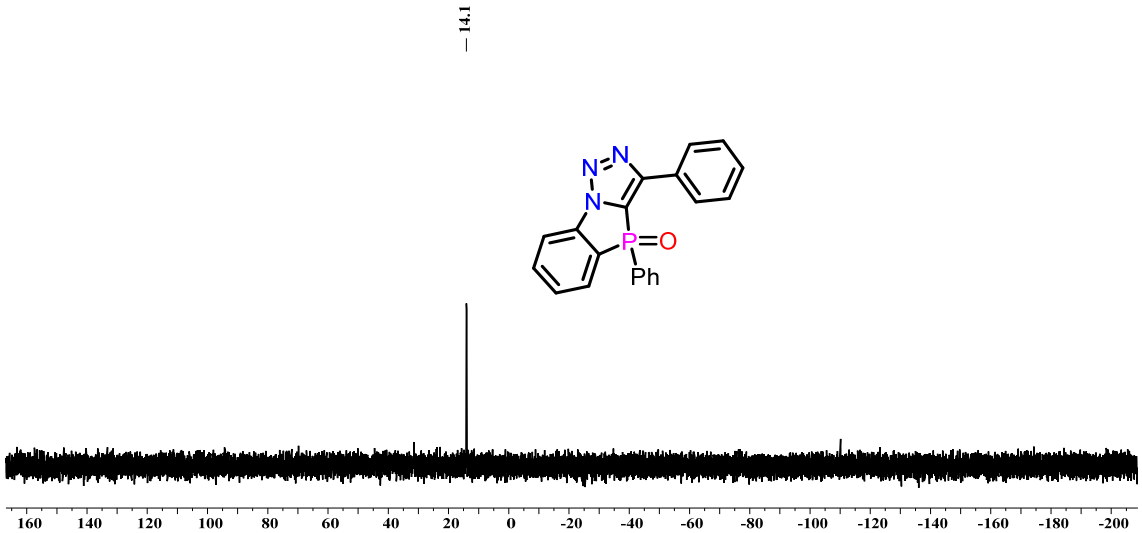

Fig. S16 $^{31}P\{^{1}H\}$ NMR spectrum of **L2o** in $CDCl_3$ (162 MHz).

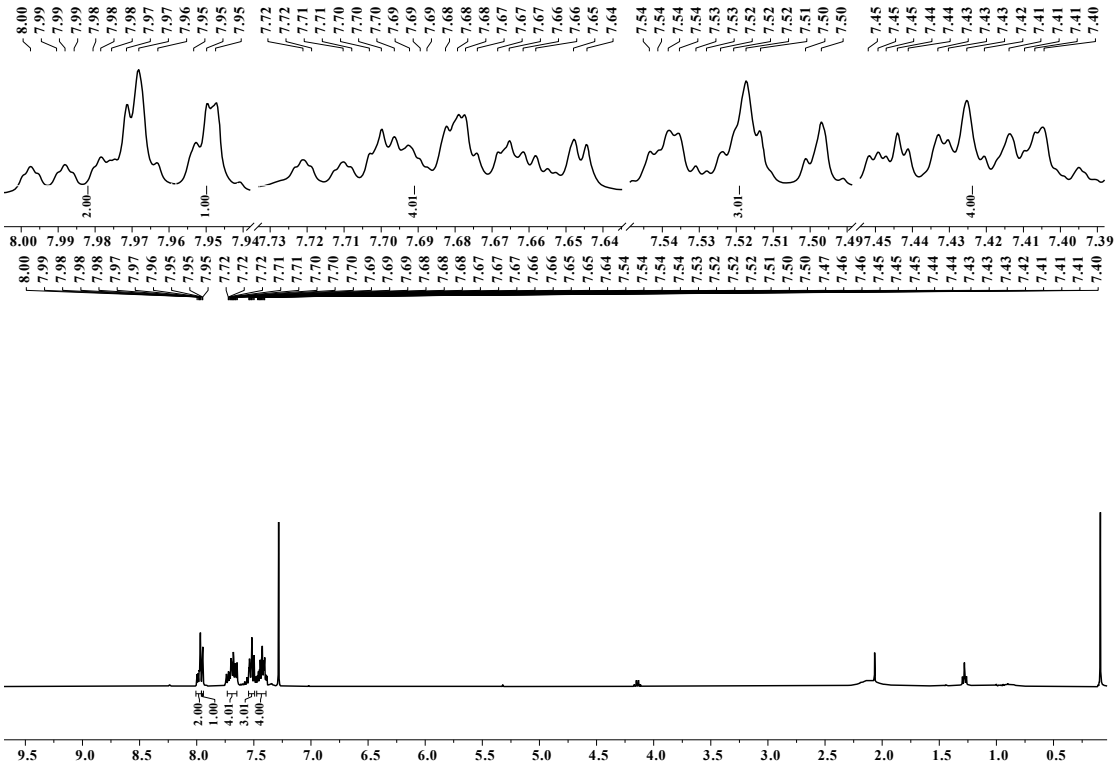

Fig. S17 ^{1}H NMR spectrum of **L2o** in $CDCl_3$ (400 MHz).

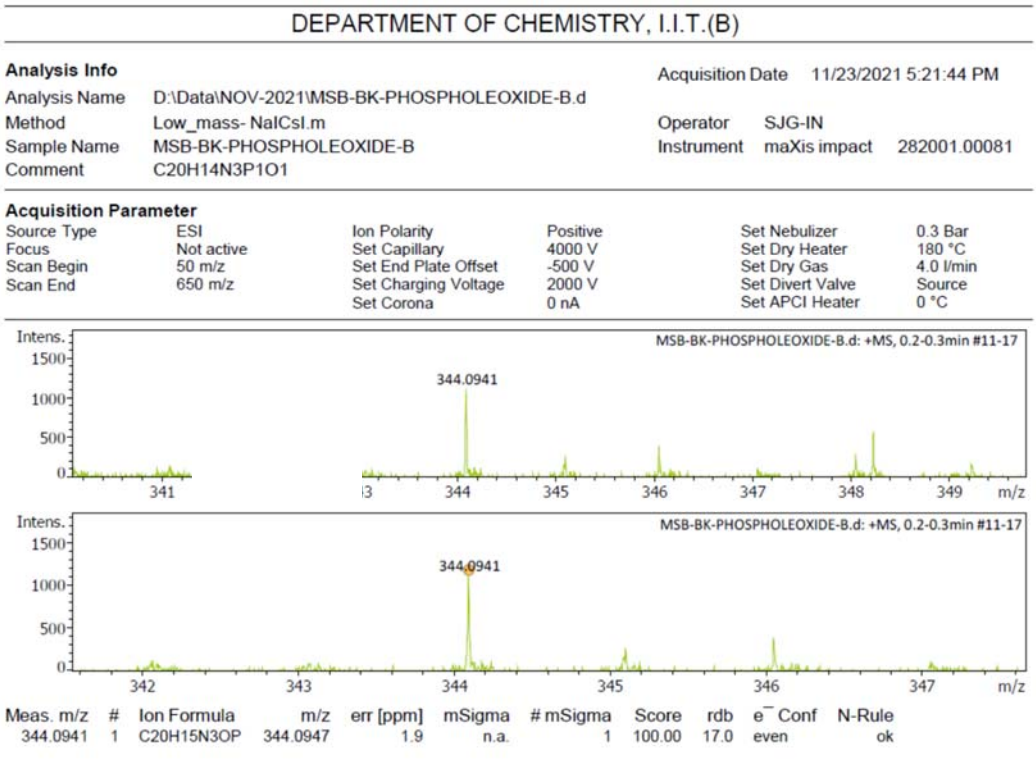

Fig. S18 HRMS spectrum of **L2o**.

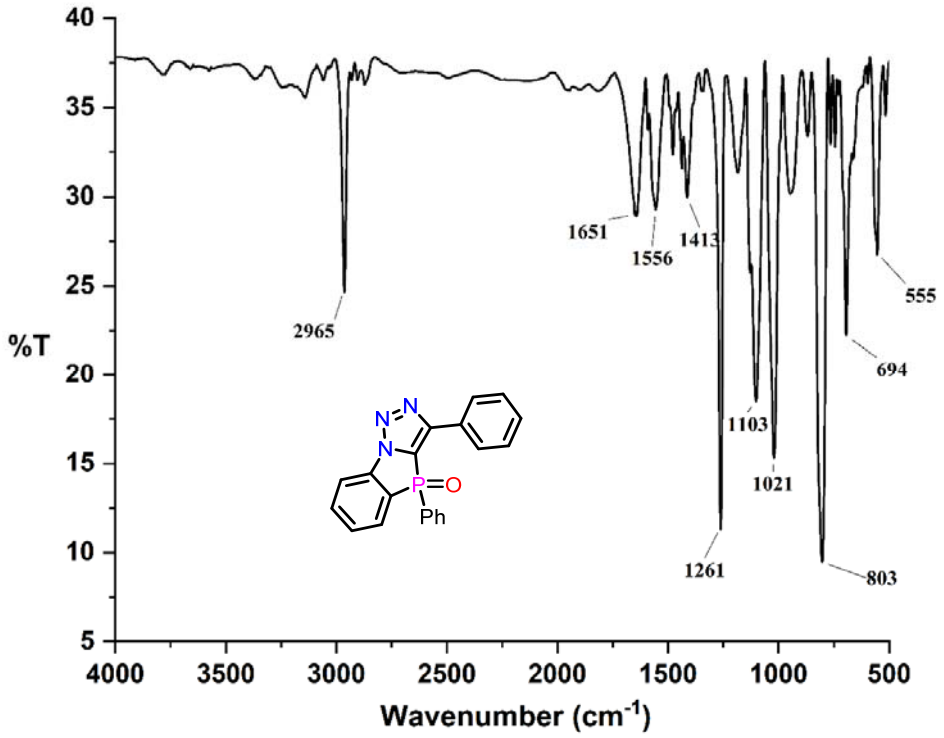

Fig. S19 FT-IR spectrum of compound $\mathbf{L2_O}$.

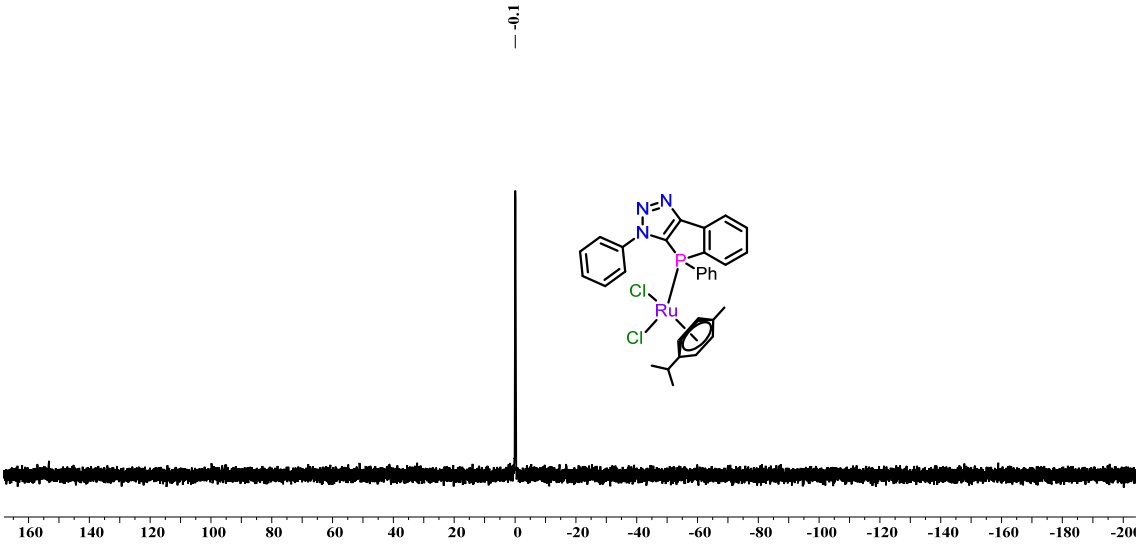

Fig. S20 $^{31}P\{^{1}H\}$ NMR spectrum of **1** in $CDCl_3$ (162 MHz).

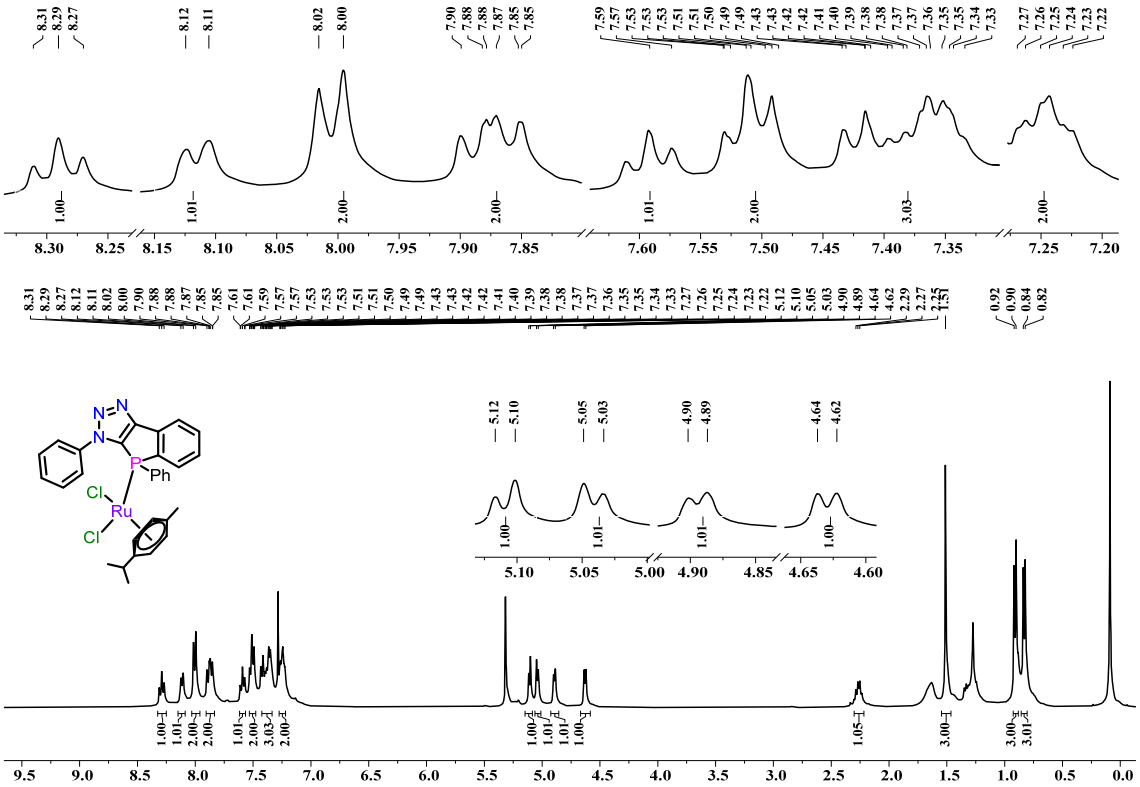

Fig. S21 ^{1}H NMR spectrum of **1** in $CDCl_3$ (400 MHz).

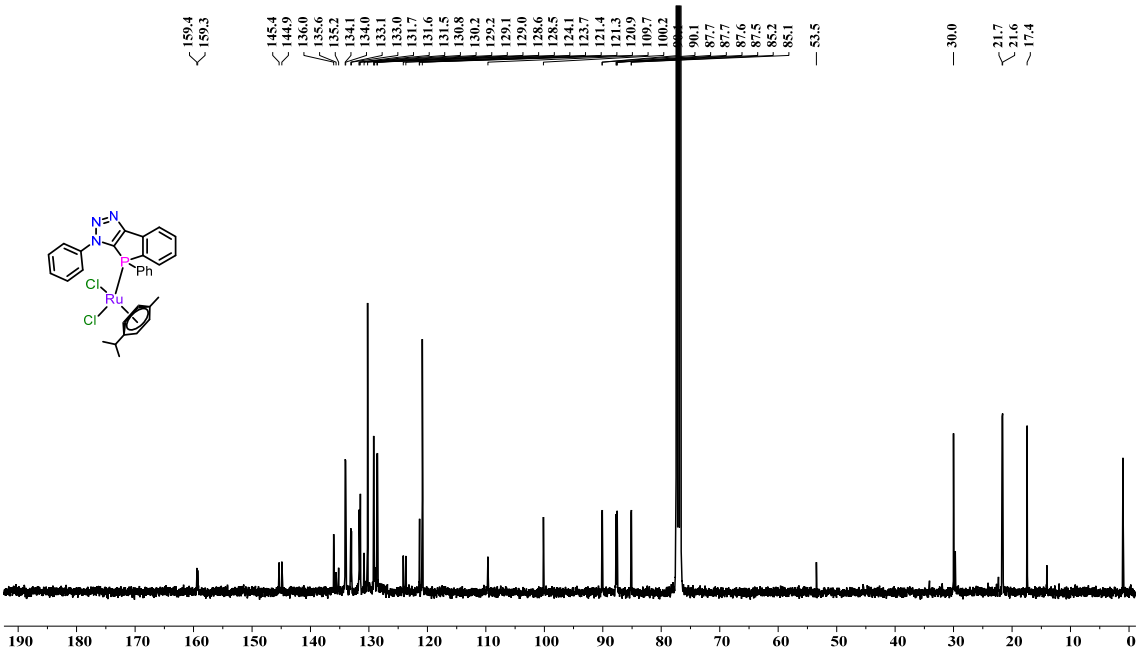

Fig. S22 $^{13}C\{^{1}H\}$ NMR spectrum of **1** in $CDCl_3$ (101 MHz).

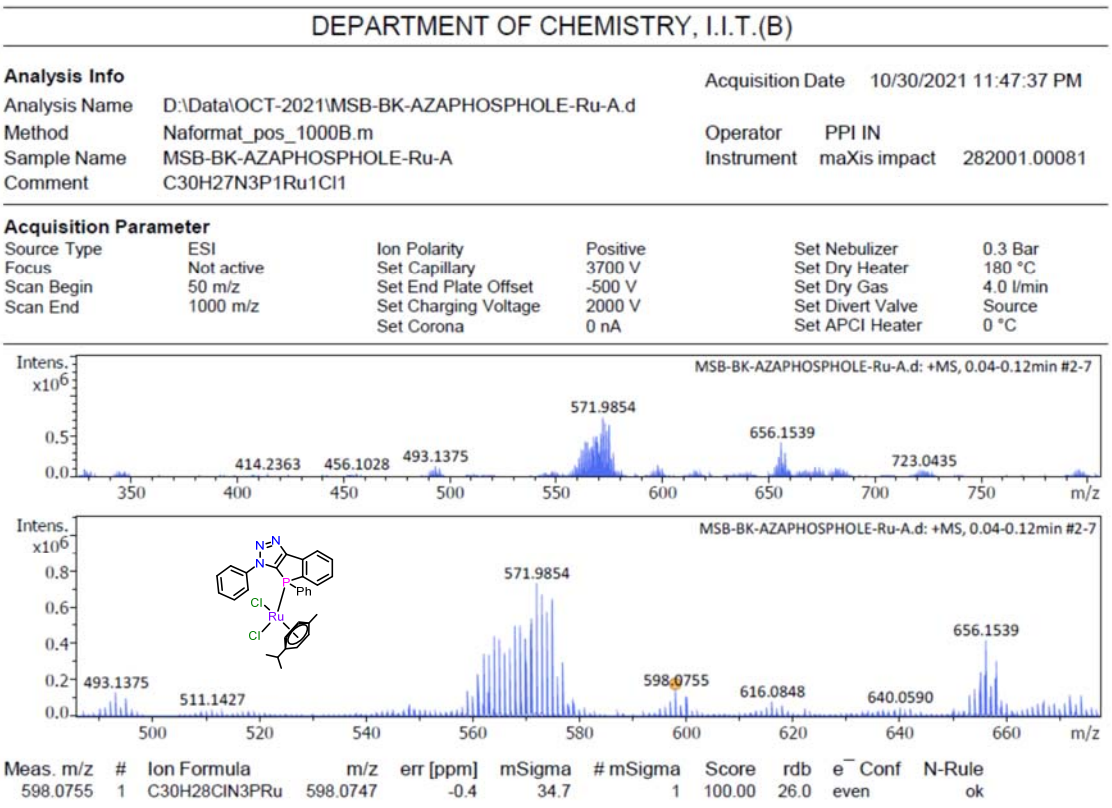

Fig. S23 HRMS spectrum of **1**.

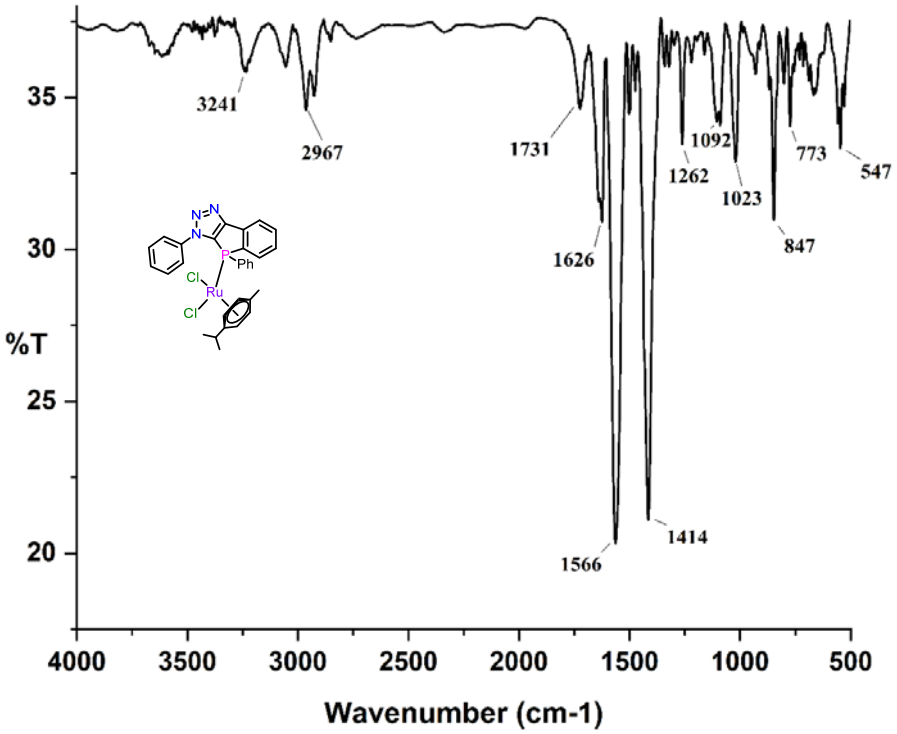

Fig. S24 FT-IR spectrum of compound **1**.

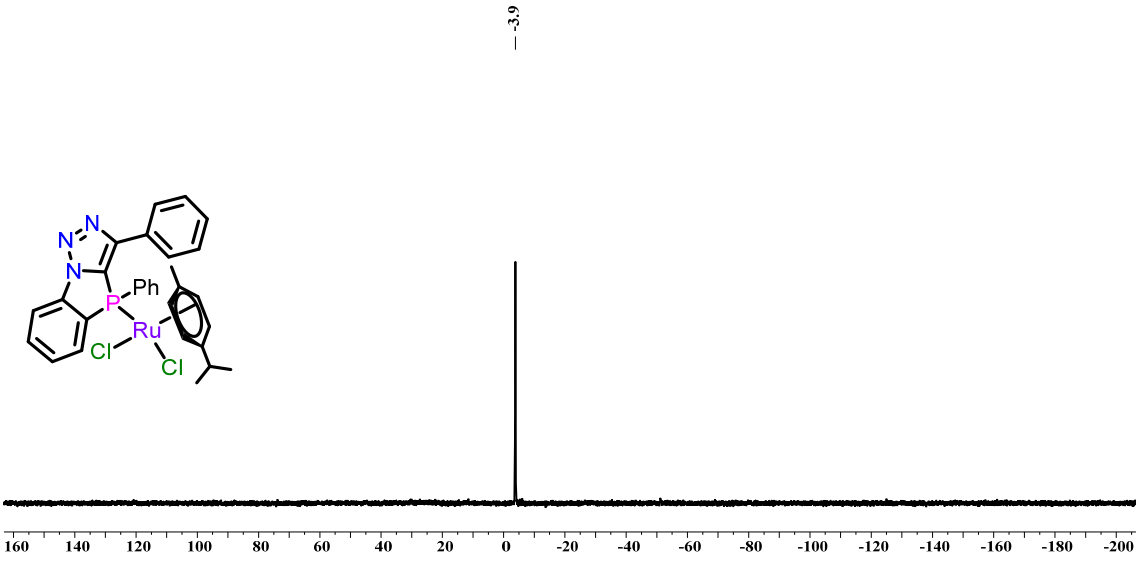

Fig. S25 $^{31}P\{^{1}H\}$ NMR spectrum of **2** in $CDCl_3$ (162 MHz).

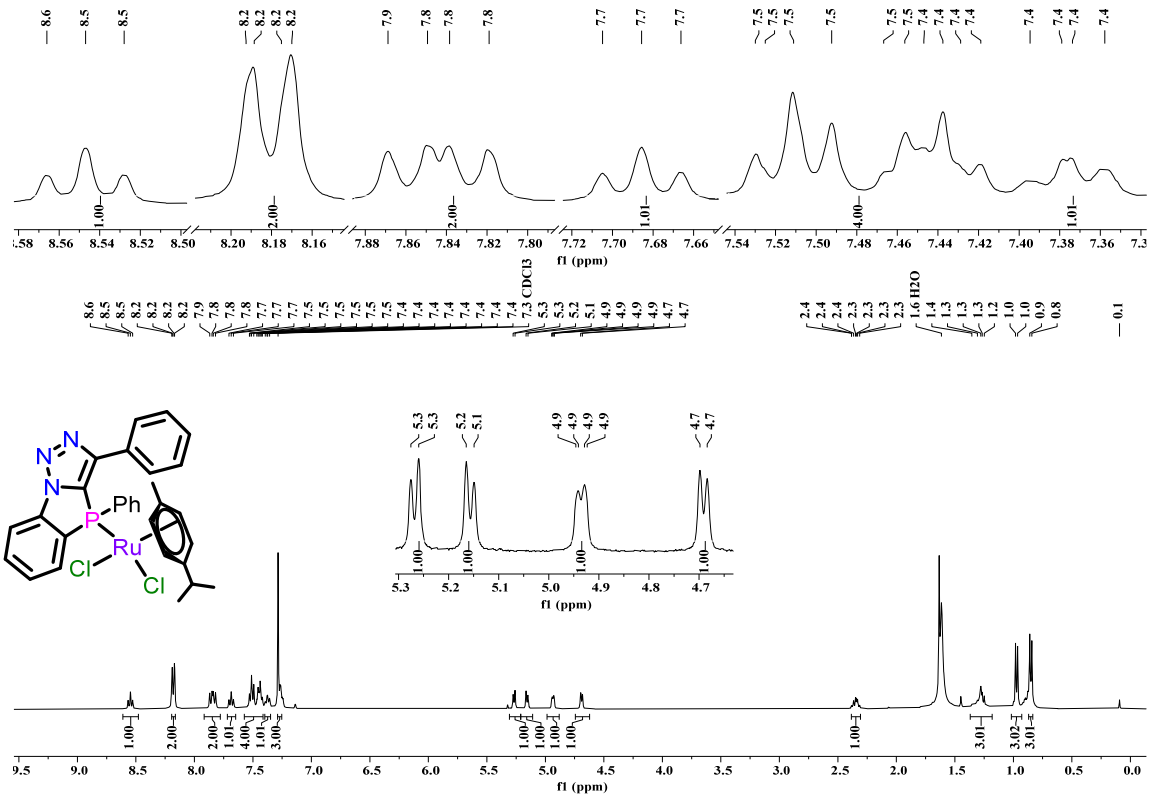

Fig. S26 ^{1}H NMR spectrum of **2** in $CDCl_3$ (400 MHz).

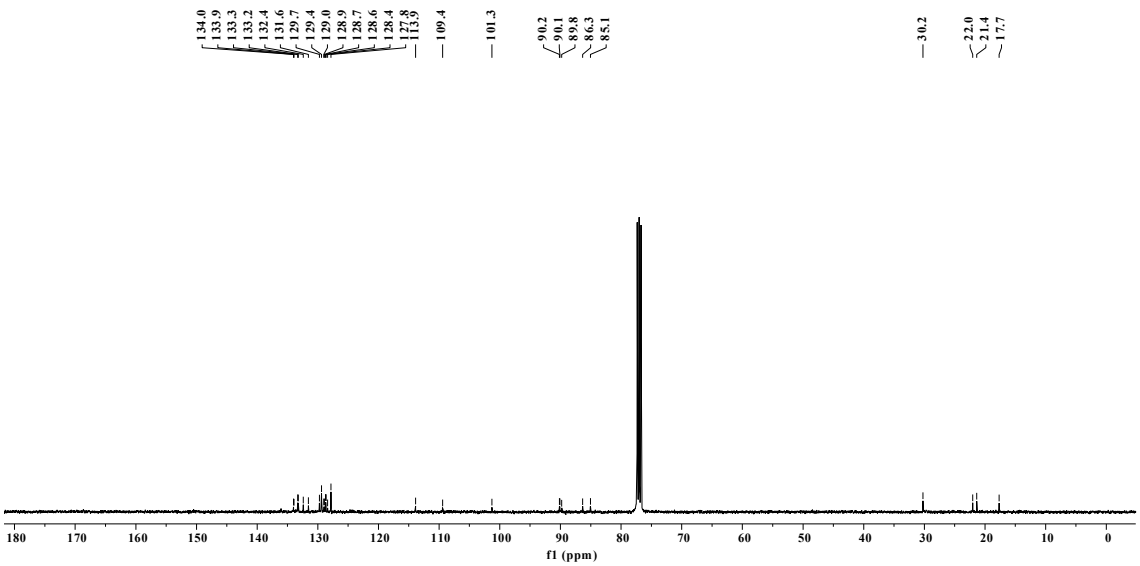

Fig. S27 $^{13}C\{^{1}H\}$ NMR spectrum of **2** in $CDCl_3$ (101 MHz).

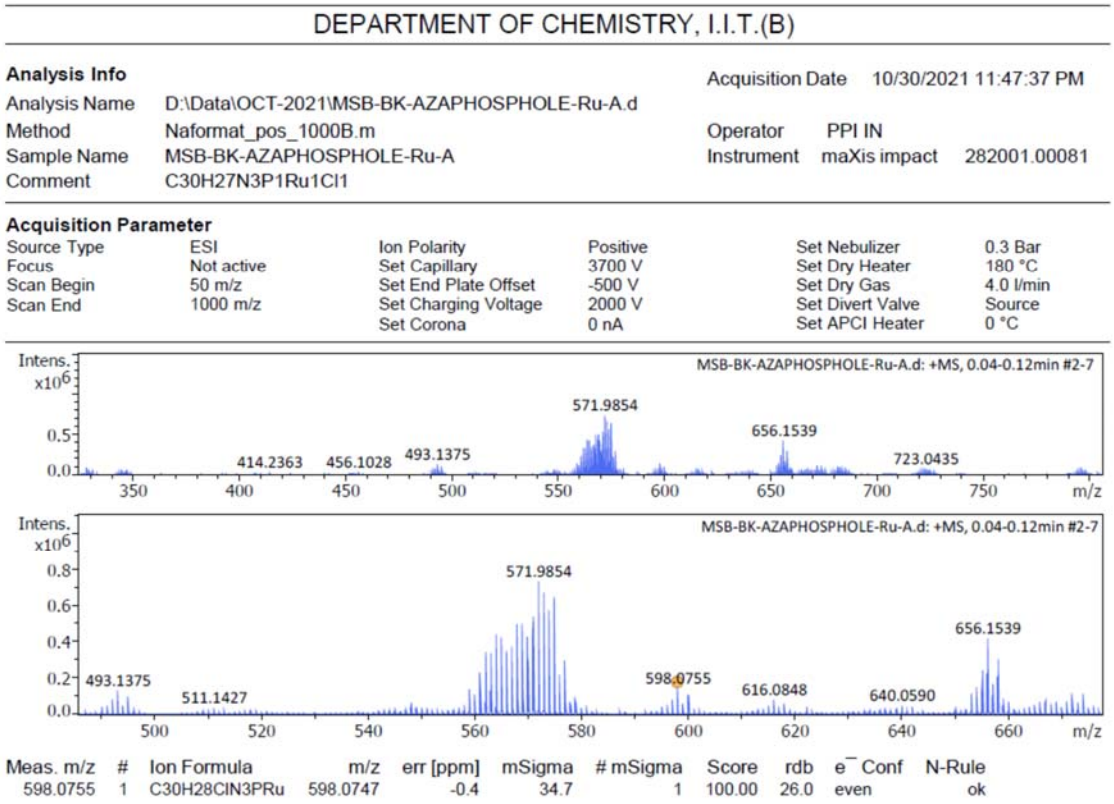

Fig. S28 HRMS spectrum of **2**.

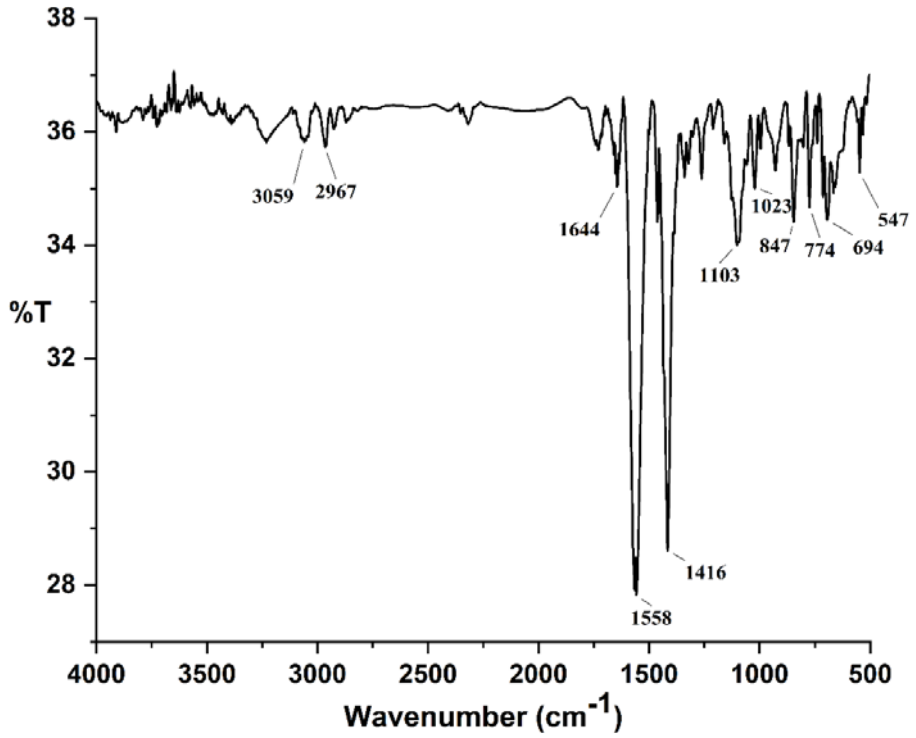

Fig. S29 FT-IR spectrum of compound **2**.

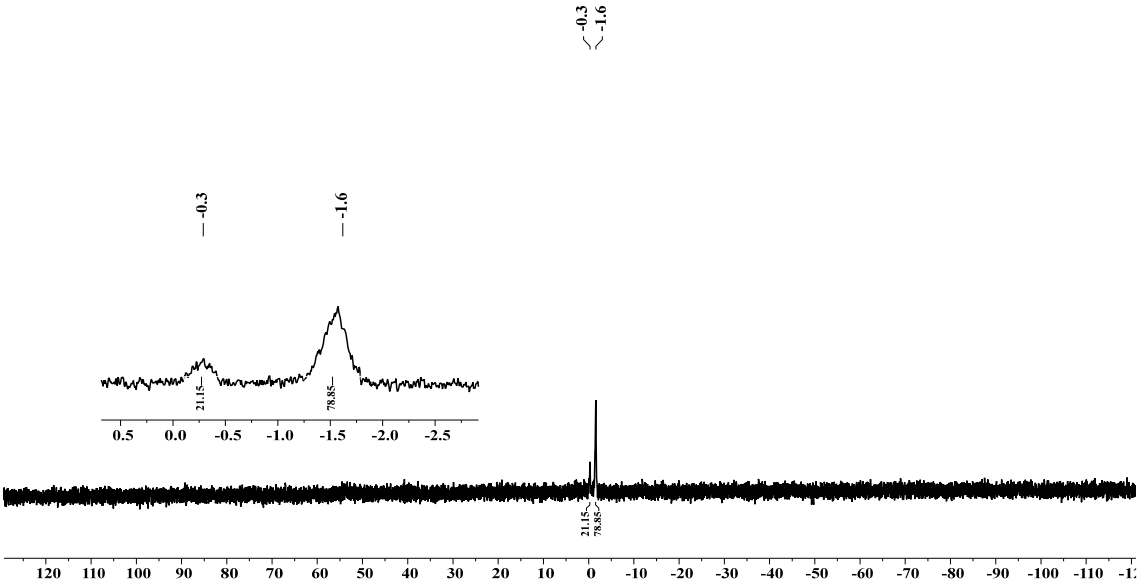

Fig. S30 $^{31}P\{^{1}H\}$ NMR spectrum of **3** in $CDCl_3$ (162 MHz).

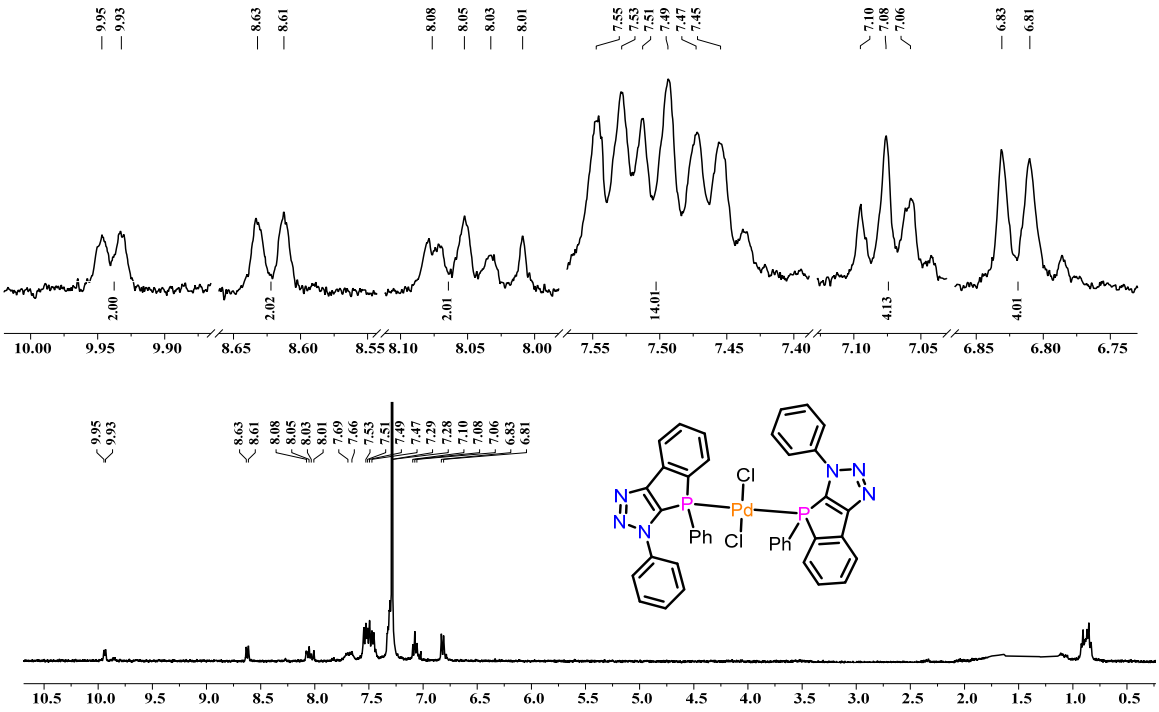

Fig. S31 ^{1}H NMR spectrum of **3** in $CDCl_3$ (400 MHz).

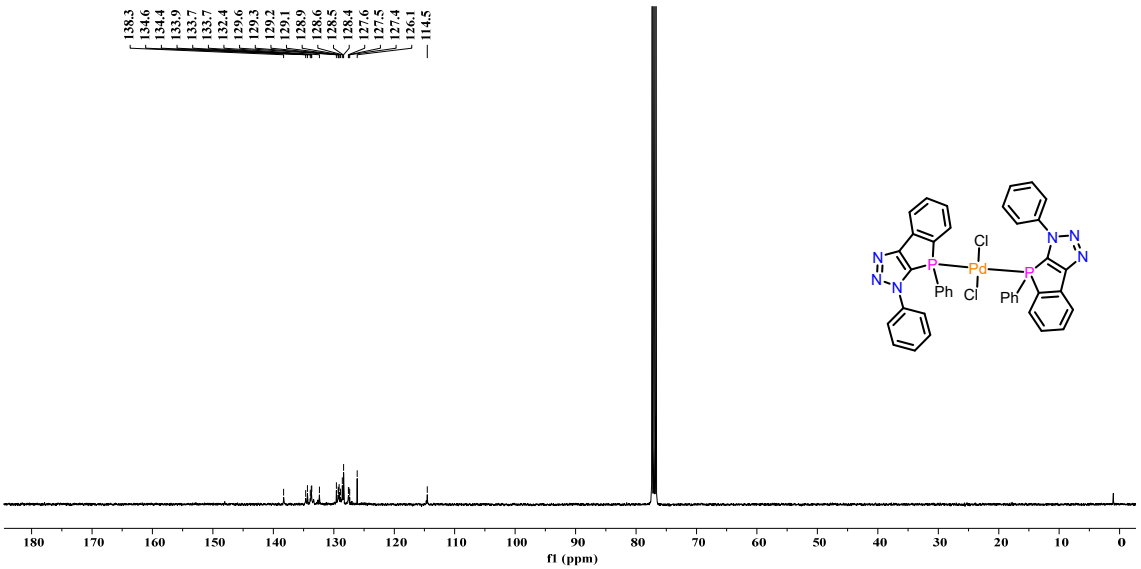

Fig. S32 $^{13}C\{^{1}H\}$ NMR spectrum of **3** in $CDCl_3$ (101 MHz).

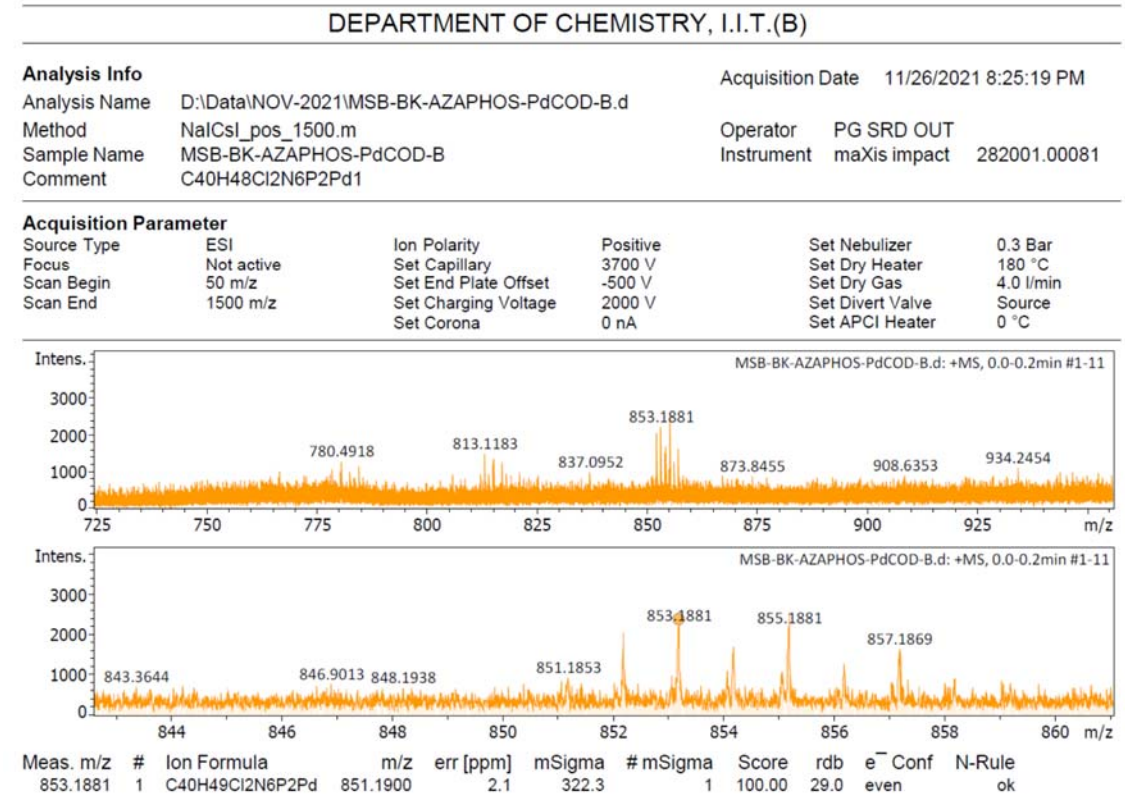

Fig. S33 HRMS spectrum of **3**.

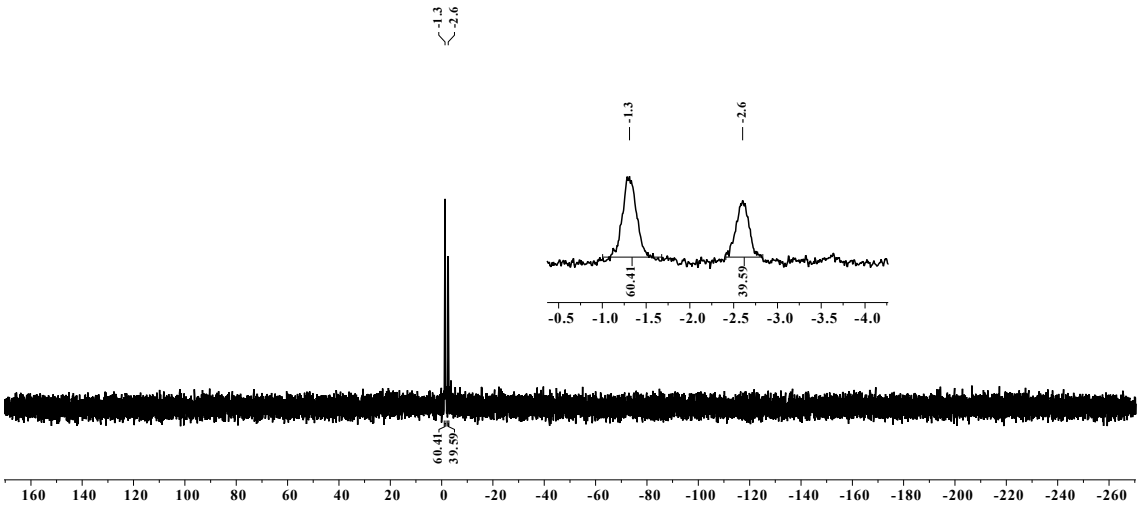

Fig. S34 $^{31}P\{^{1}H\}$ NMR spectrum of **4** in $CDCl_3$ (162 MHz).

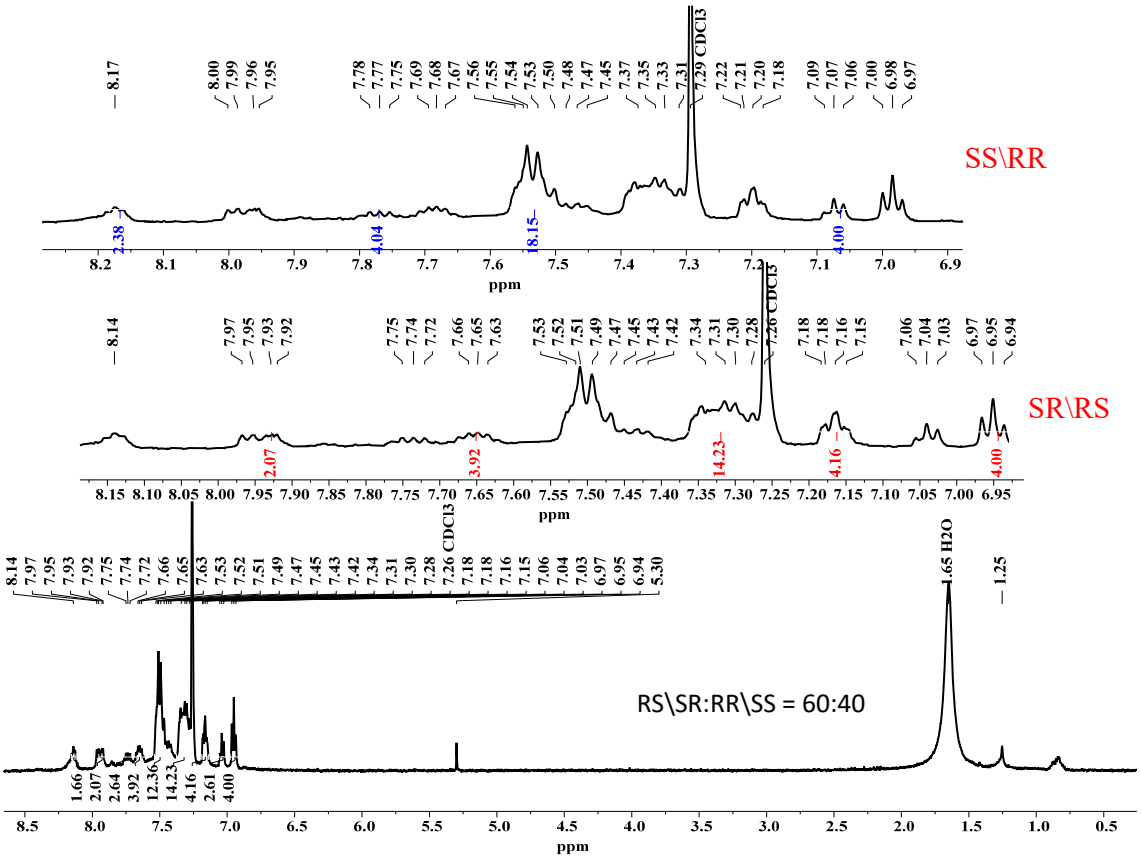

Fig. S35 ^{1}H NMR spectrum of **4** in $CDCl_3$ (400 MHz).

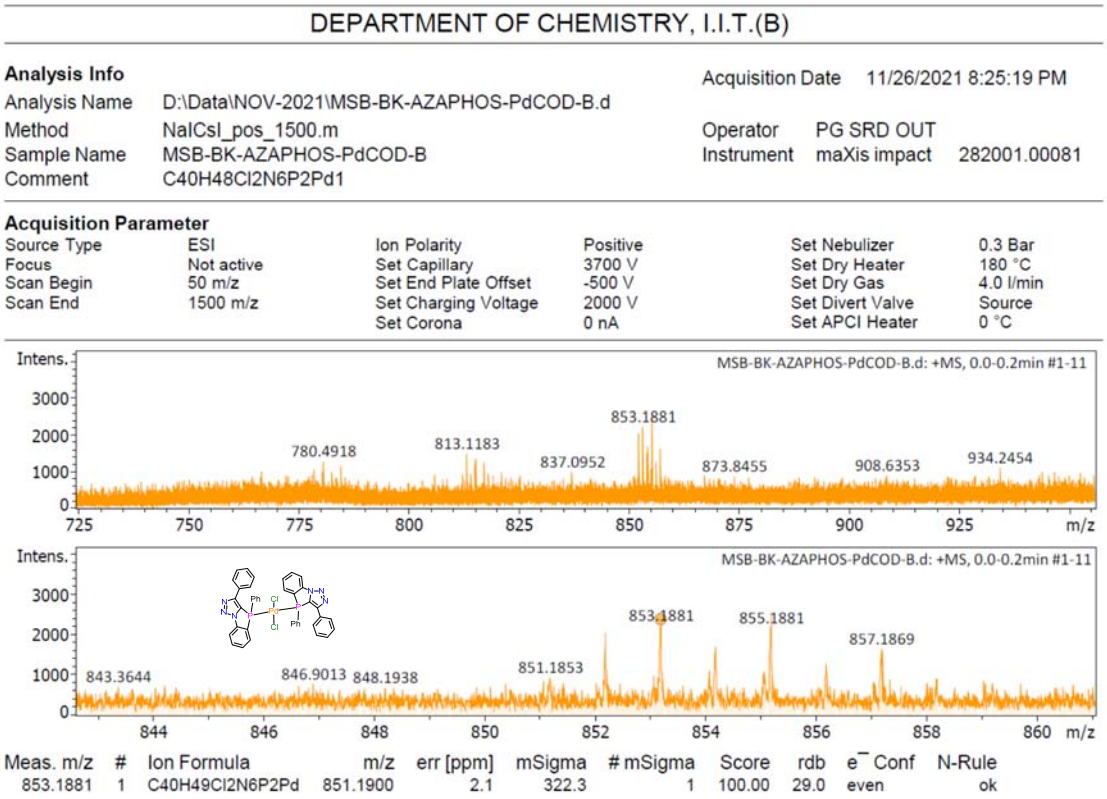

Fig. S36 HRMS spectrum of **4**.

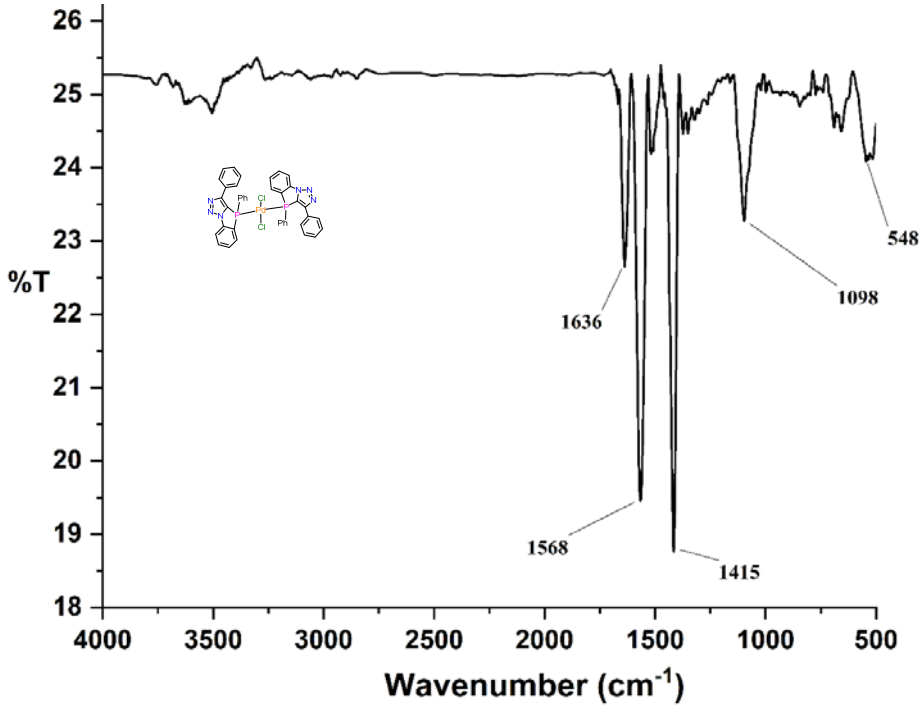

Fig. S37 FT-IR spectrum of compound **4**.

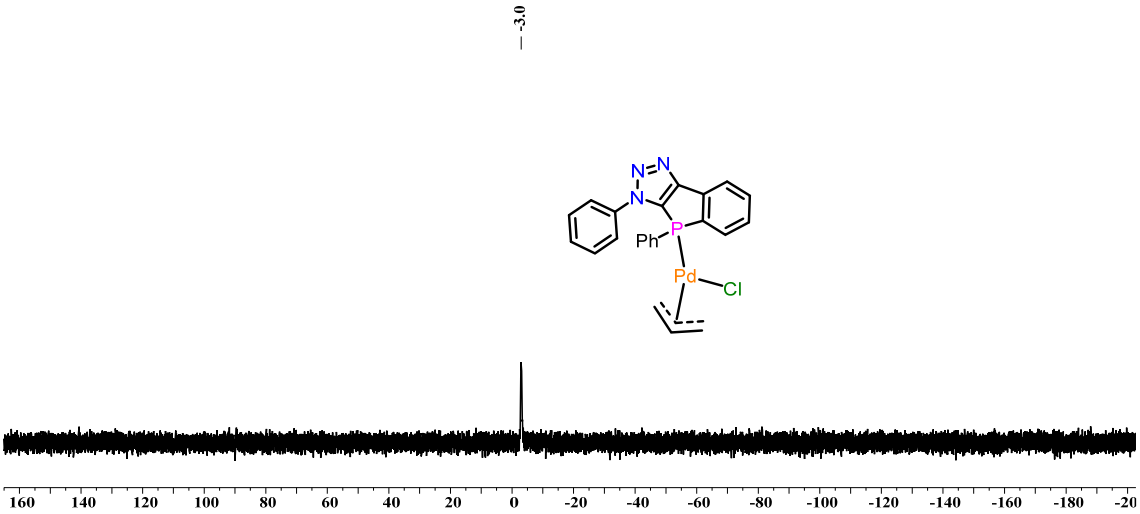

Fig. S38 $^{31}P\{^{1}H\}$ NMR spectrum of **5** in $CDCl_3$ (162 MHz).

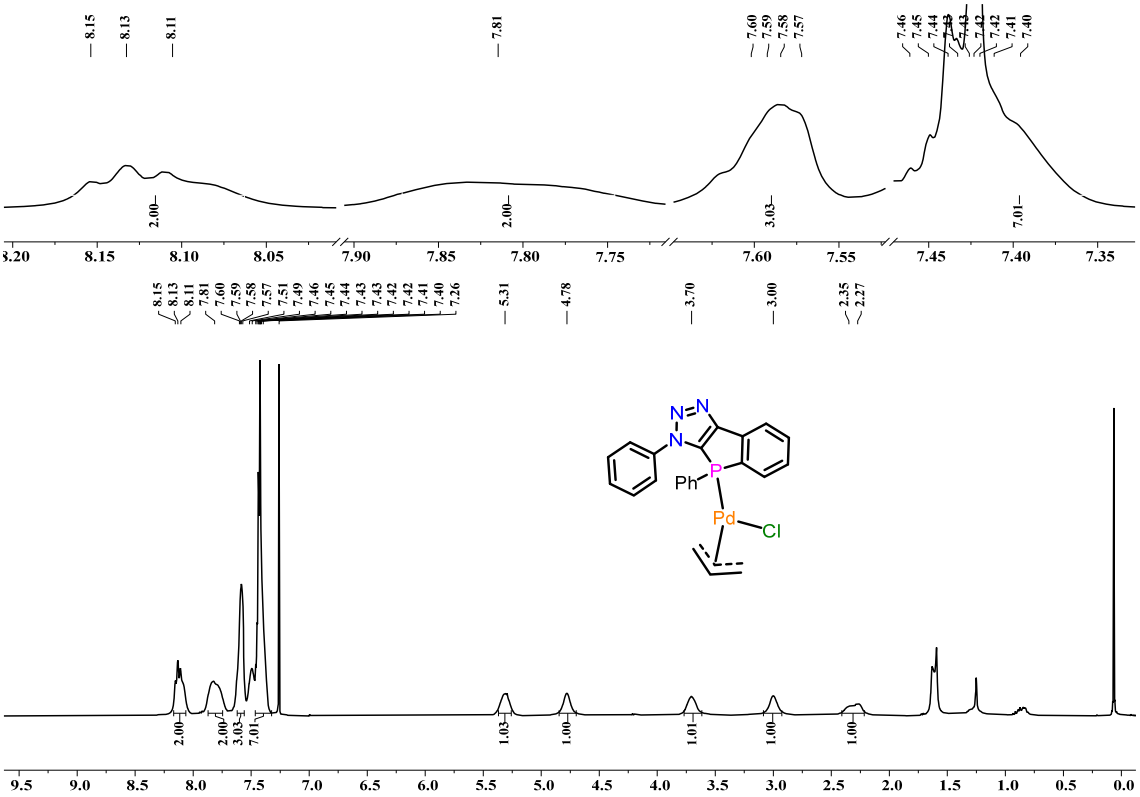

Fig. S39 ^{1}H NMR spectrum of **5** in $CDCl_3$ (400 MHz).

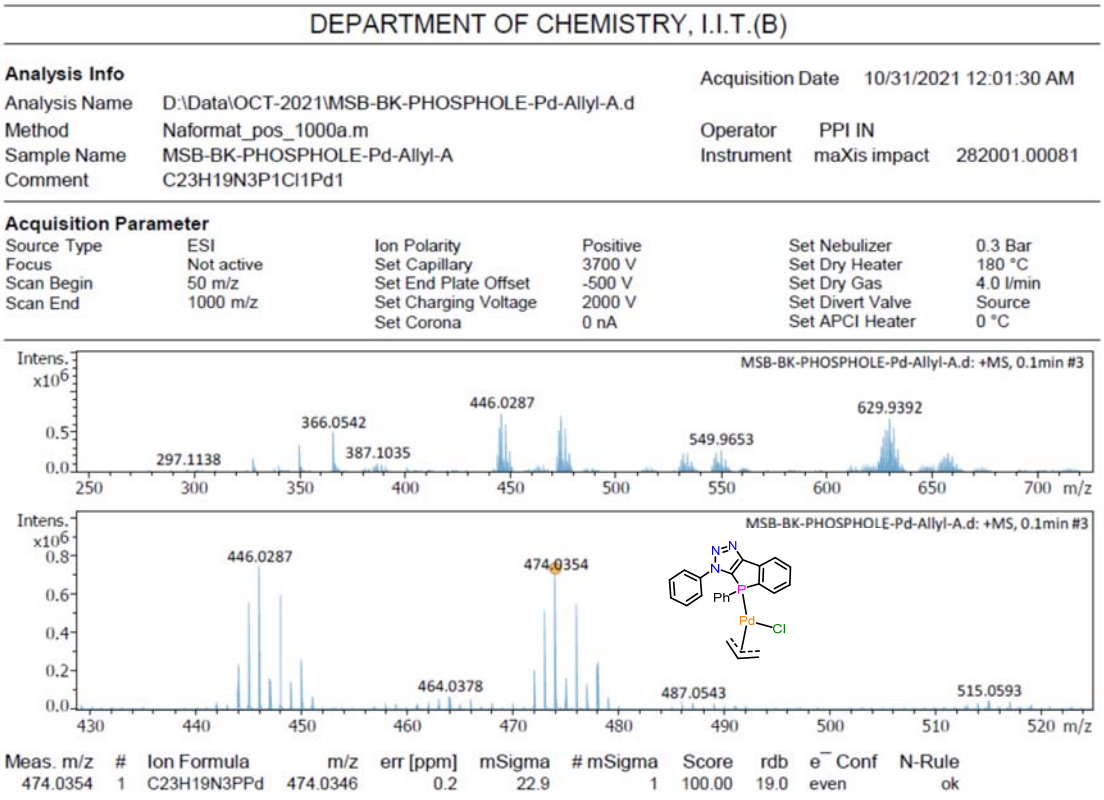

Fig. S40 HRMS spectrum of **5**.

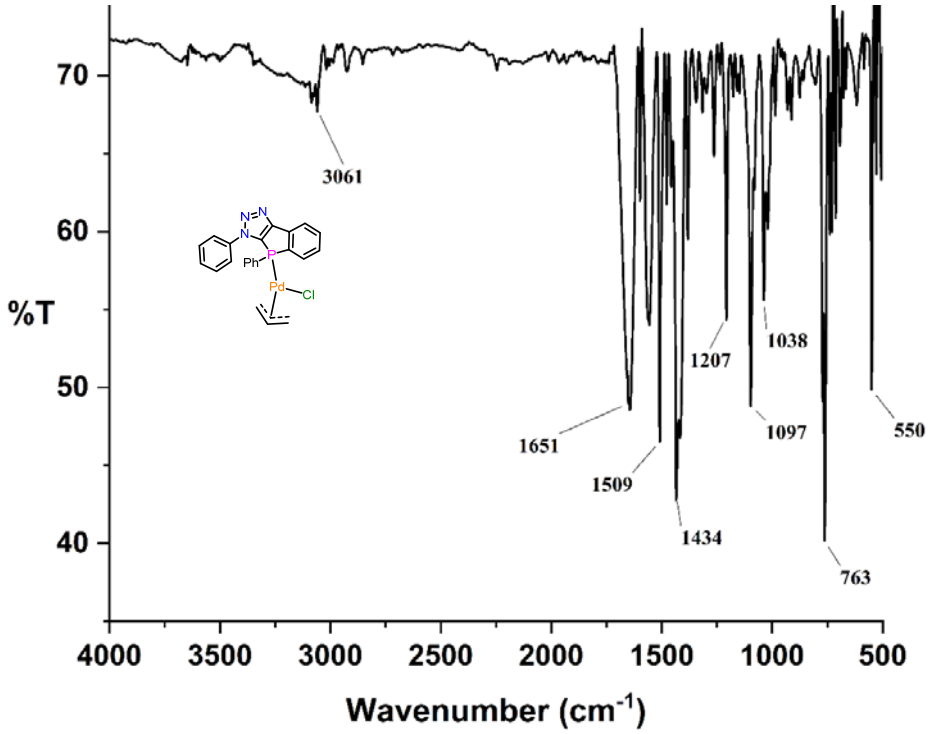

Fig. S41 FT-IR spectrum of compound **5**.

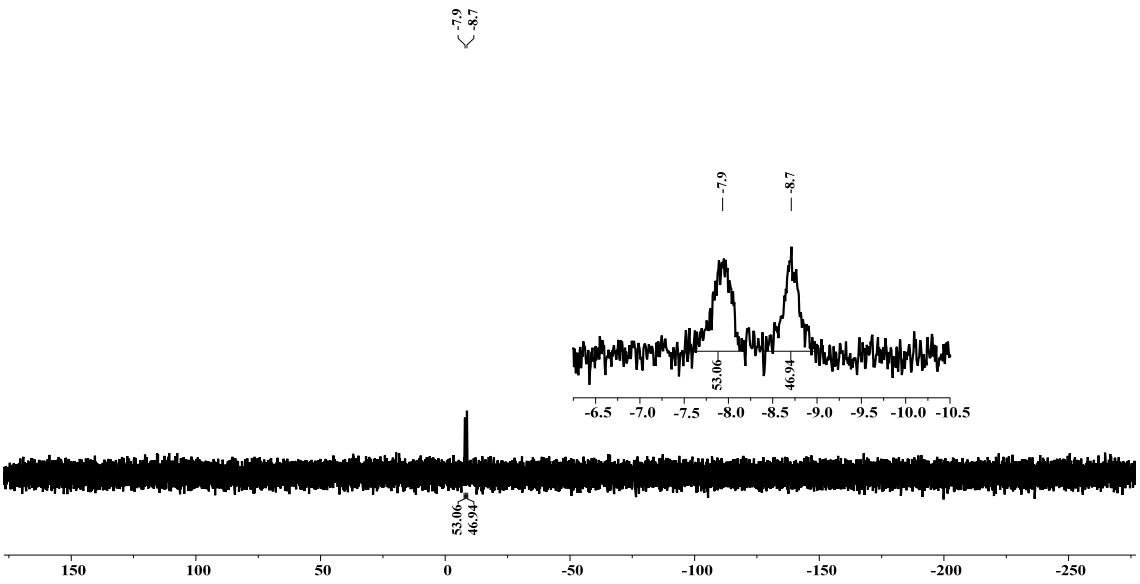

Fig. S42 $^{31}P\{^{1}H\}$ NMR spectrum of **6** in $CDCl_3$ (162 MHz).

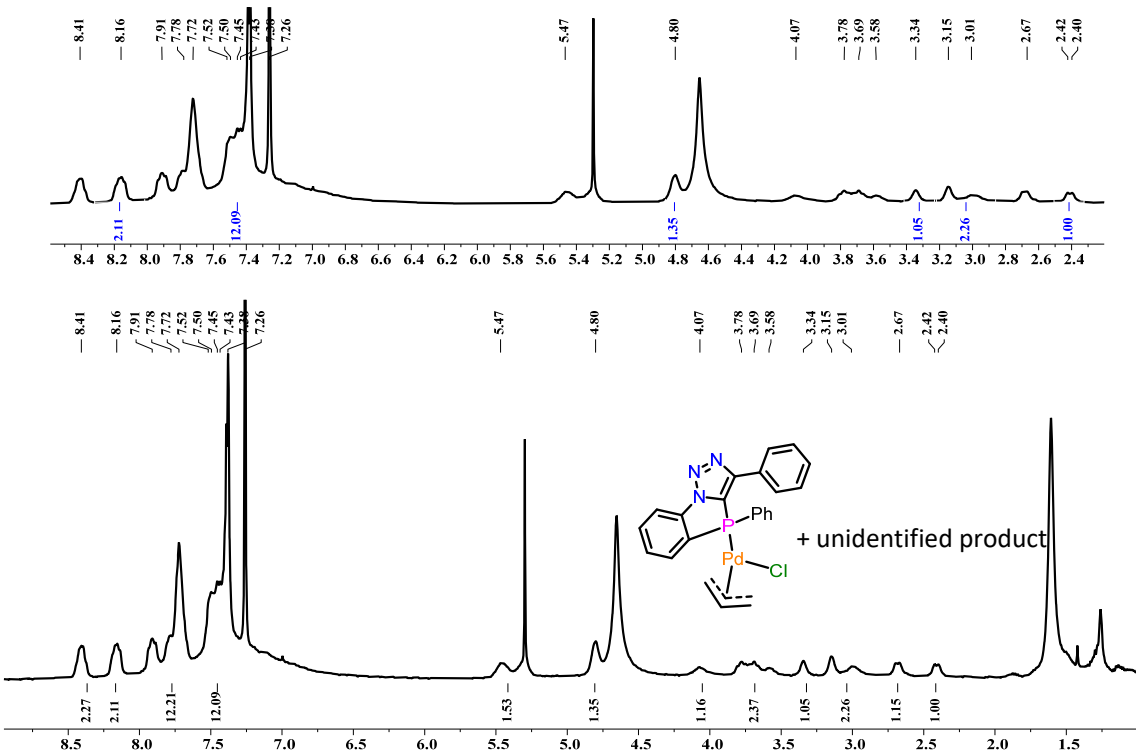

Fig. S43 ^{1}H NMR spectrum of **6** in $CDCl_3$ (400 MHz).

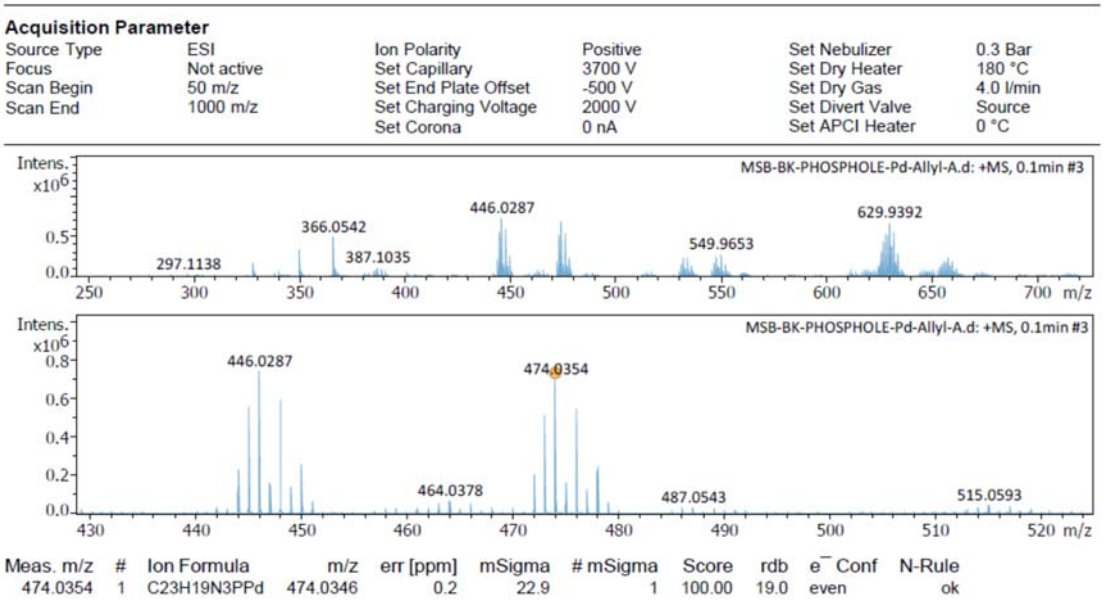

Fig. S44 HRMS spectrum of **6**.

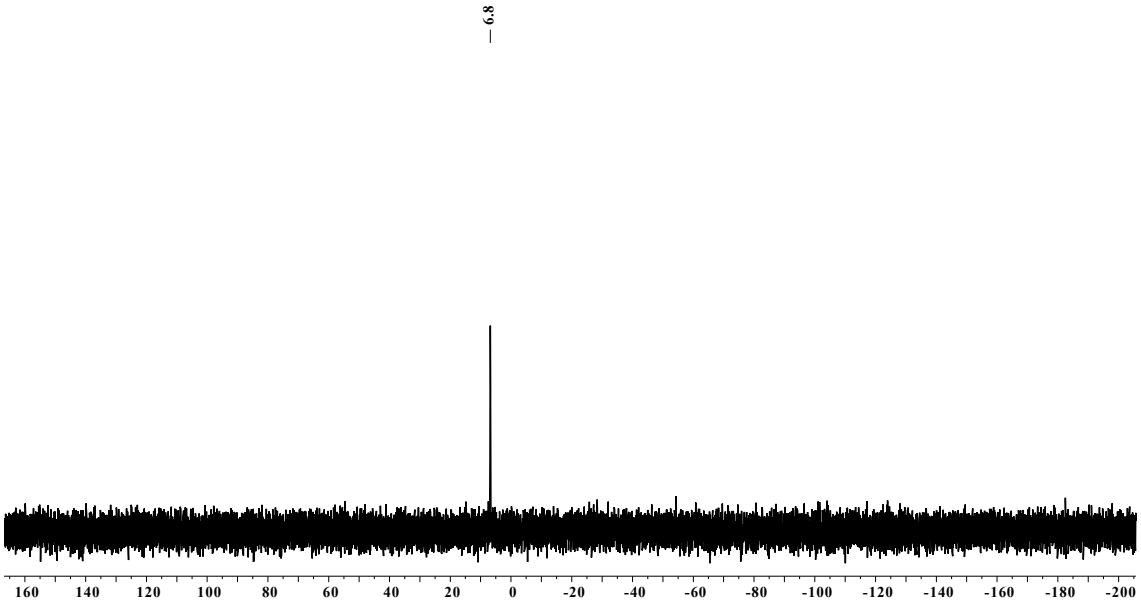

Fig. S45 $^{31}P\{^{1}H\}$ NMR spectrum of **7** in $CDCl_3$ (162 MHz).

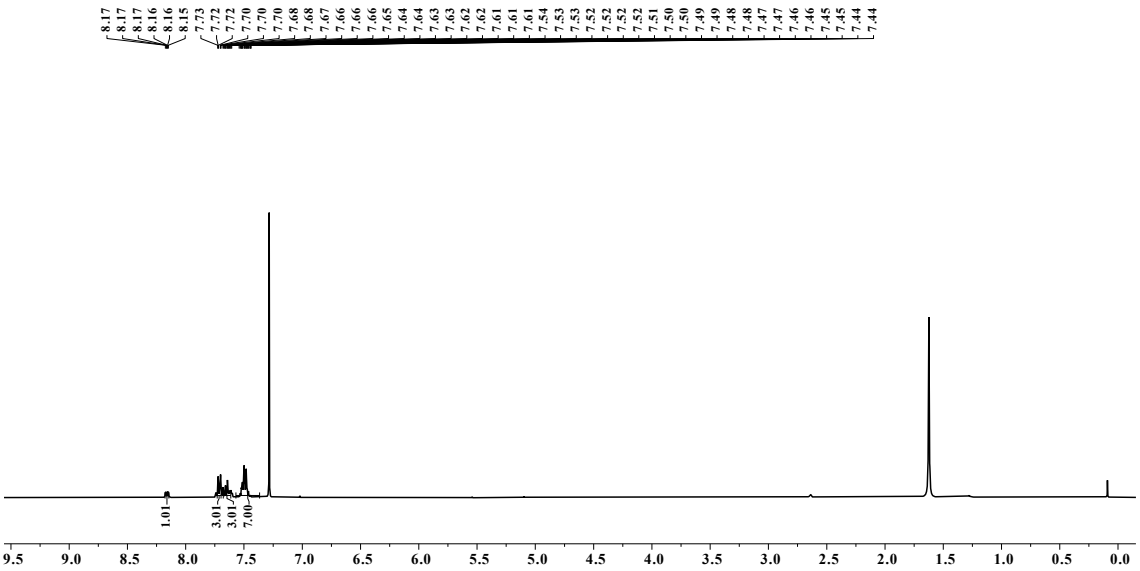

Fig. S46 ^{1}H NMR spectrum of **7** in $CDCl_3$ (400 MHz).

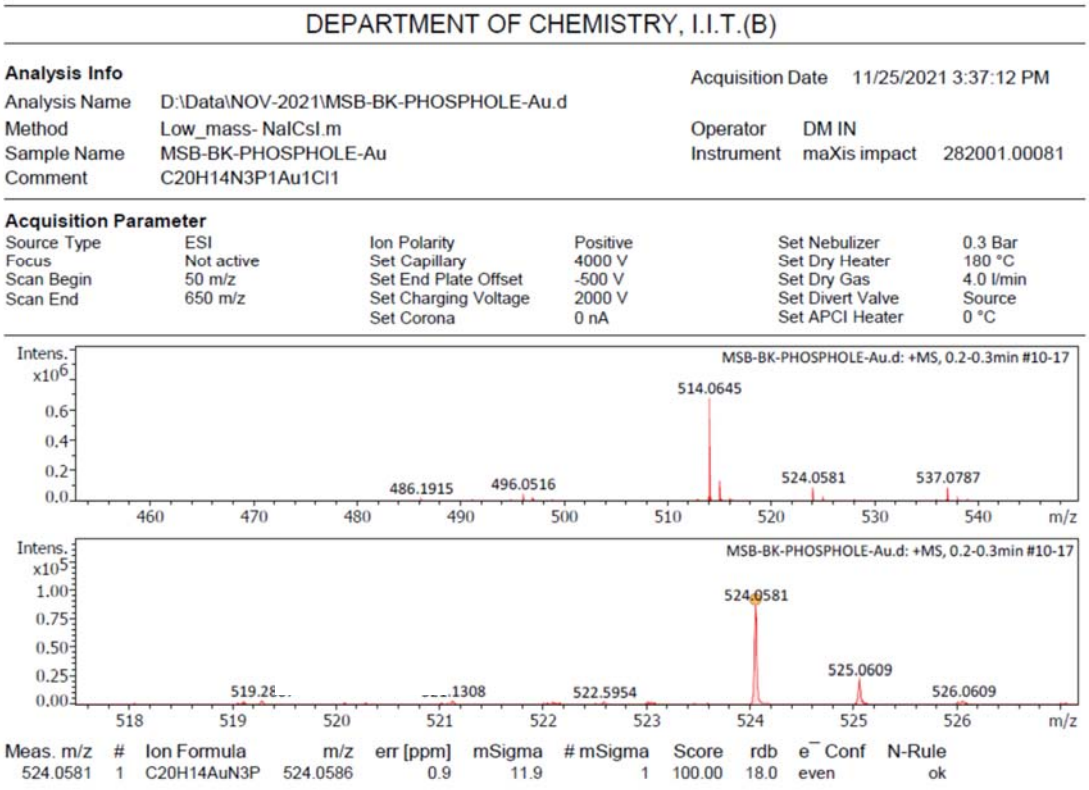

Fig. S47 HRMS spectrum of **7**.

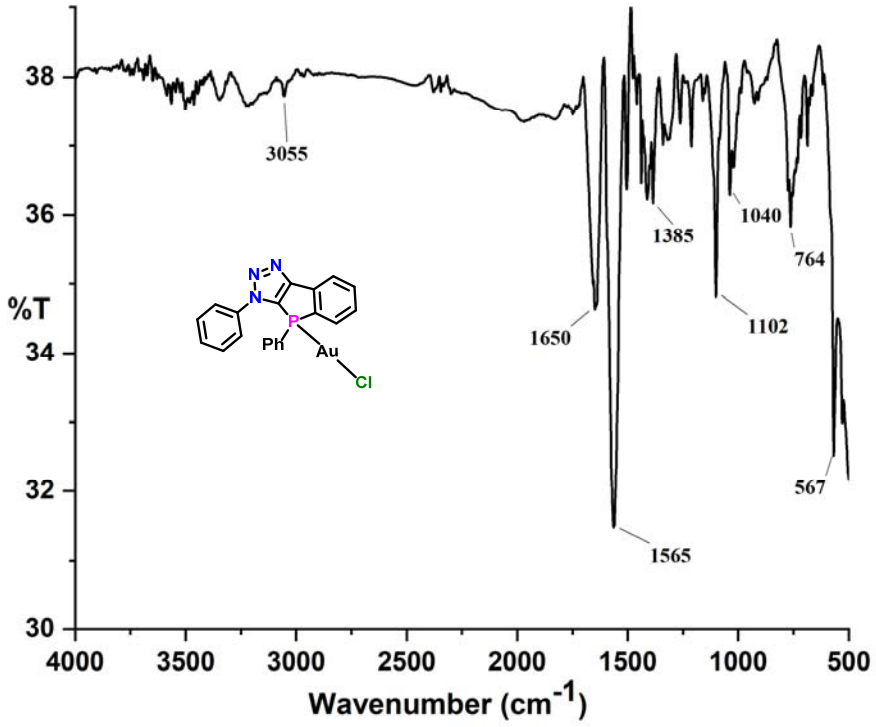

Fig. S48 FT-IR spectrum of compound **7**.

Controlled experiment

Procedure for the radical trapping experiment

Diphenylmethane (1.0 mmol), **1** (0.5 mol%), TBHP (4.0 mmol) and TEMPO (4.0 mmol) were added to 2 mL of CH_2Cl_2 in a 5 mL reaction tube. The solution was stirred at room temperature for 2 h under open atmosphere. After the completion of reaction GC-MS analysis reveal the formation of benzyl alcohol-TEMPO adduct.

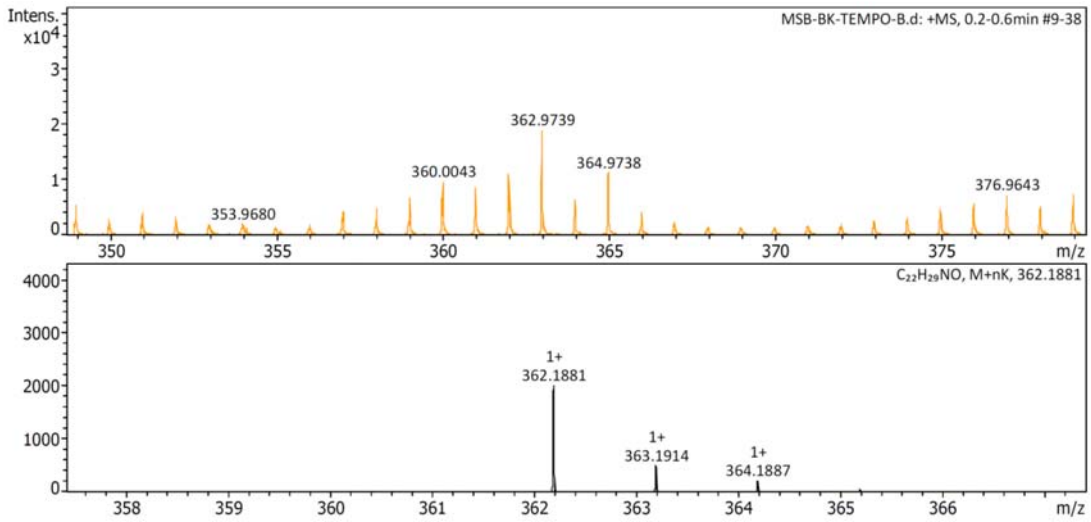

Fig. S49 LRMS spectrum of the intermediate trapping by TEMPO.

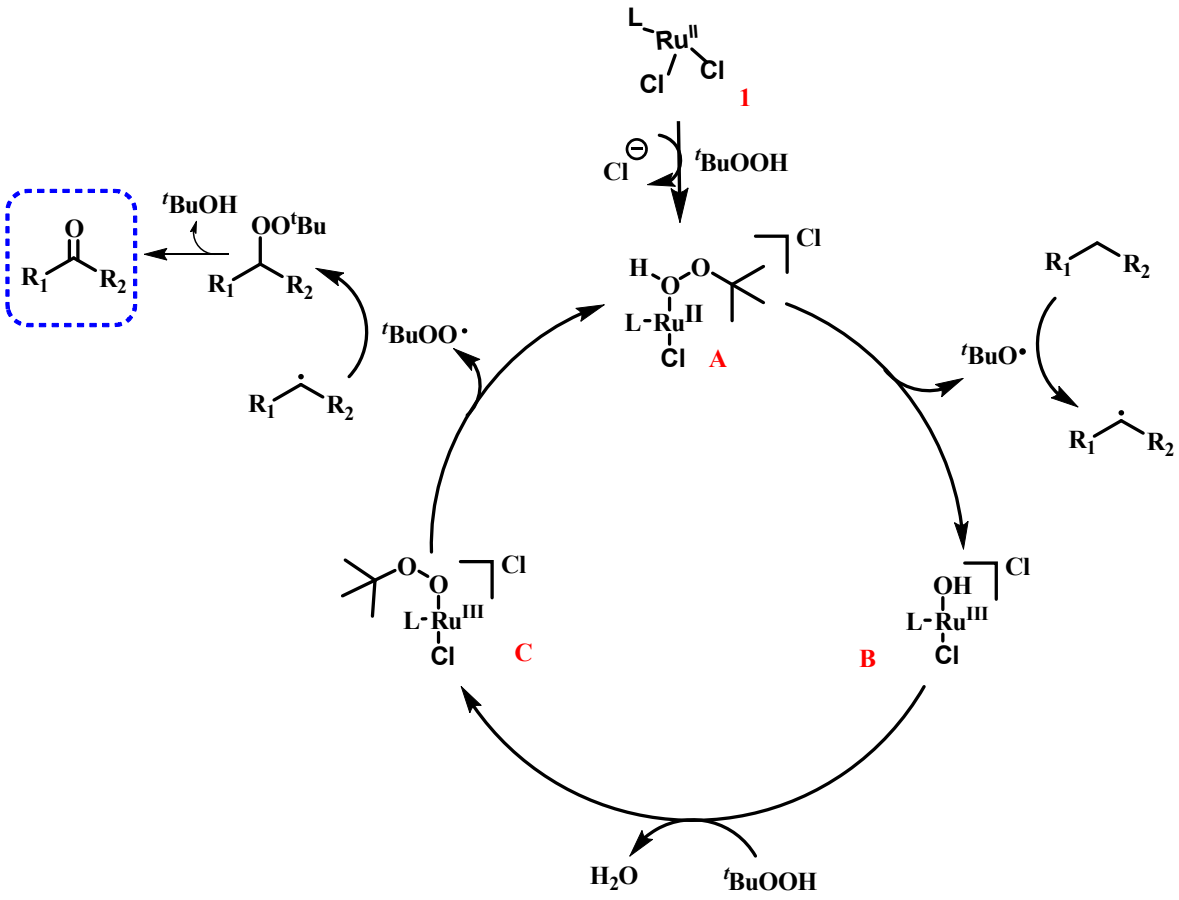

Scheme S1 Plausible Ru^{II}-catalyzed benzylic C−H oxidation cycle.

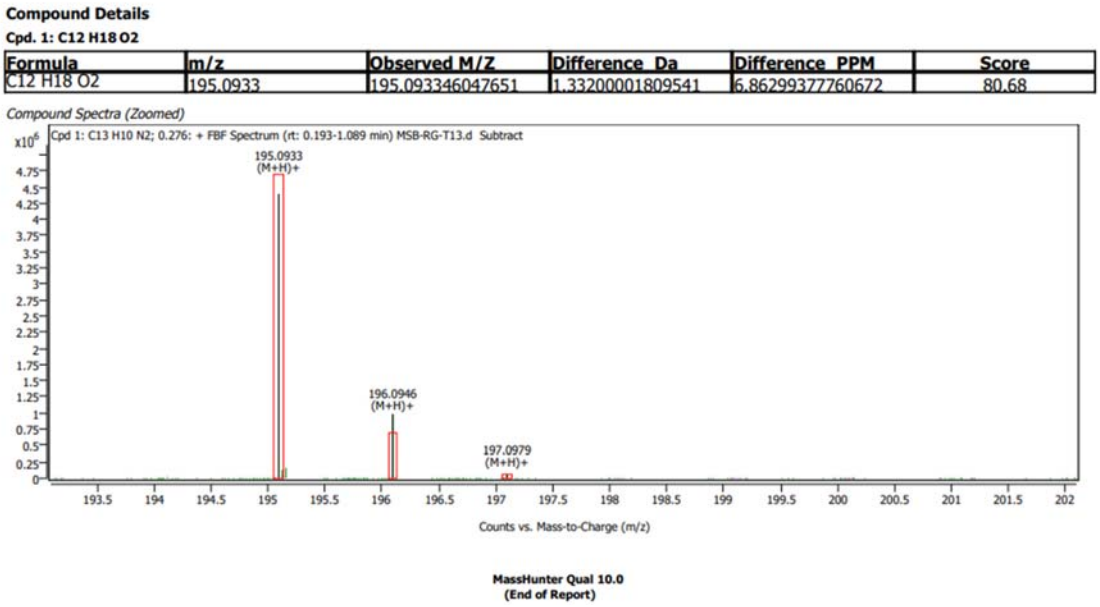

Fig. 50 LRMS for oxygenated intermediate

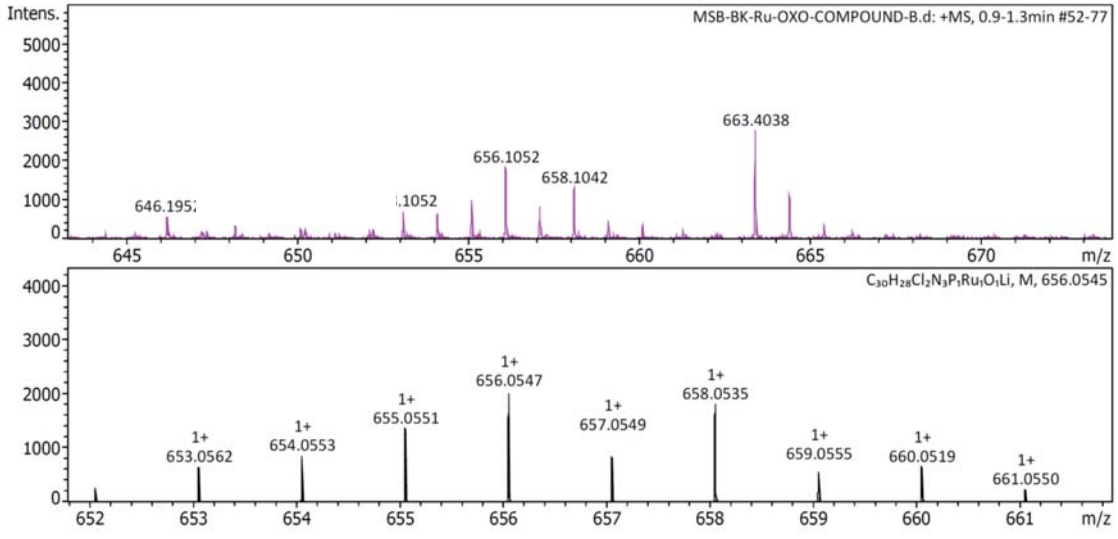

Fig. 51 LRMS spectrum of the intermediate Ru^{III} (**B**).

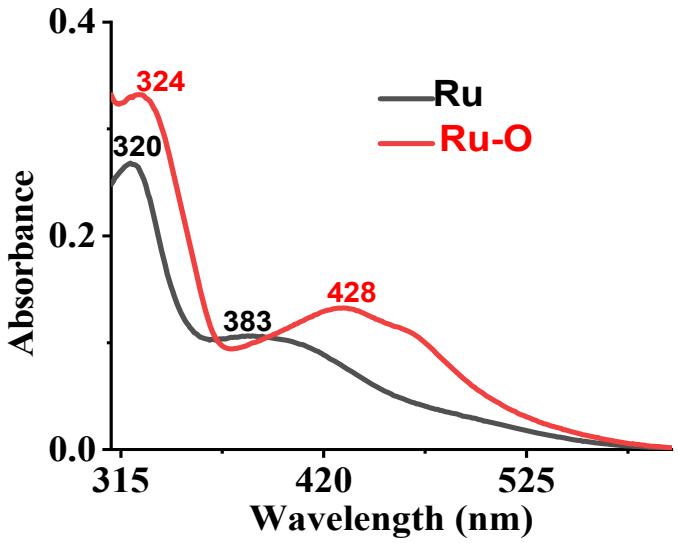

Fig. 52 UV−Vis absorption spectrum of **1** (1×10^{-5} M) with TBHP (0.1 mol/L) in CH_2Cl_2 at rt changed the spectrum from Ru^{II} (black) to Ru^{III} (red).

NMR spectra of catalytic products

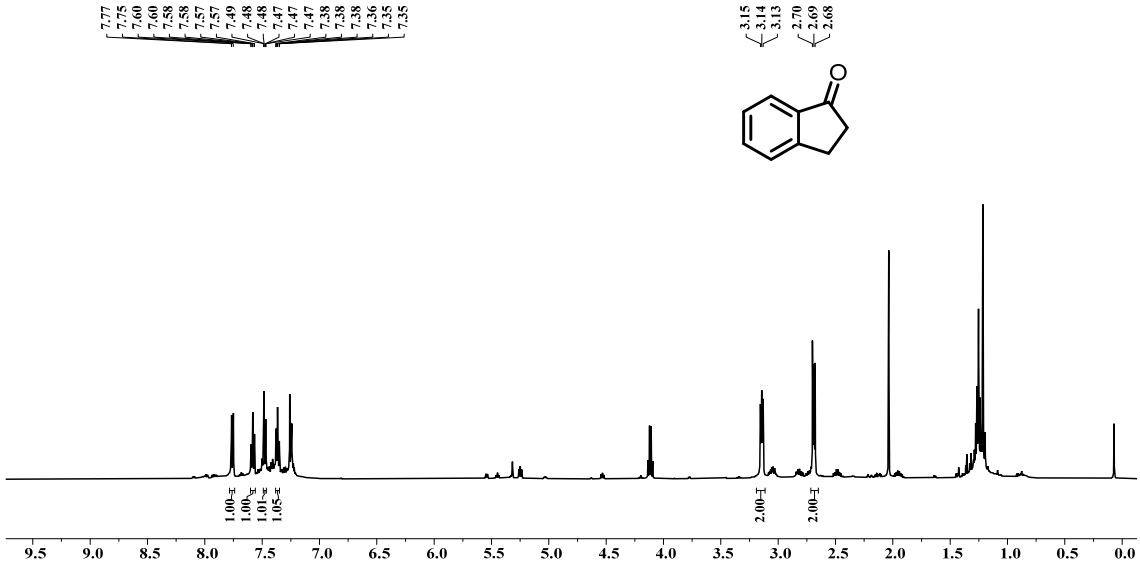

Fig. S53 ^{1}H NMR spectrum of **1a** in $CDCl_3$ (500 MHz).

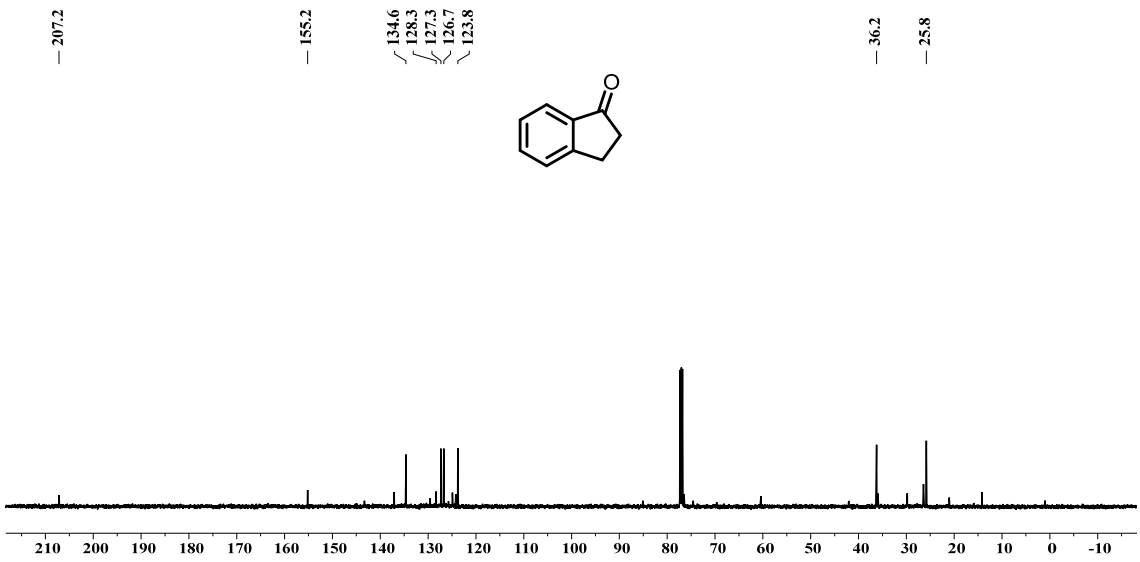

Fig. S54 $^{13}C\{^{1}H\}$ NMR spectrum of **1a** in $CDCl_3$ (126 MHz).

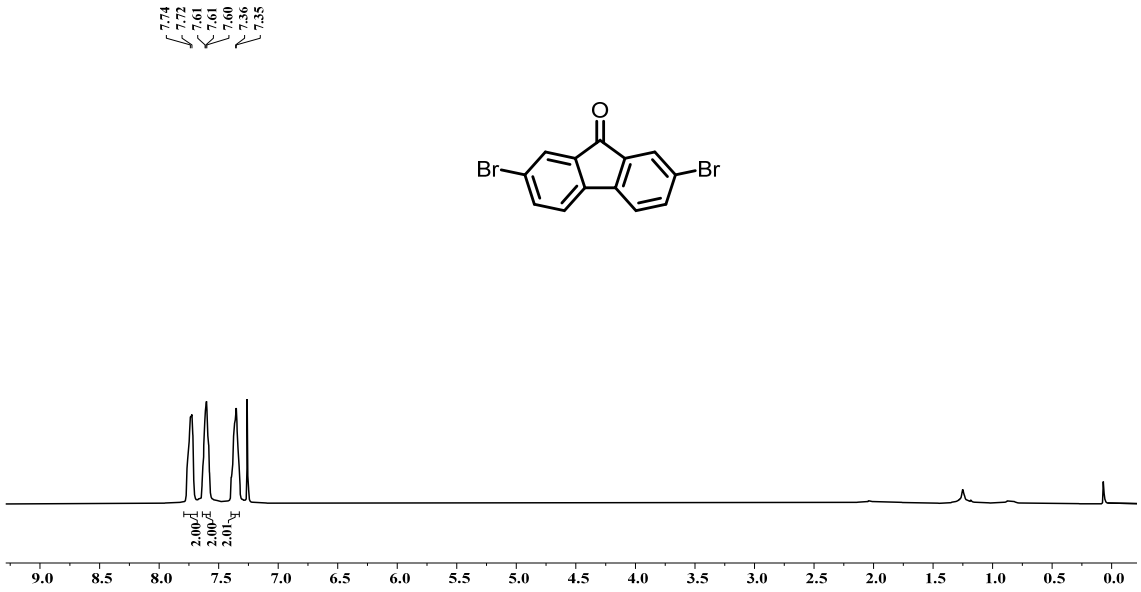

Fig. S55 ^{1}H NMR spectrum of **1b** in $CDCl_3$ (400 MHz).

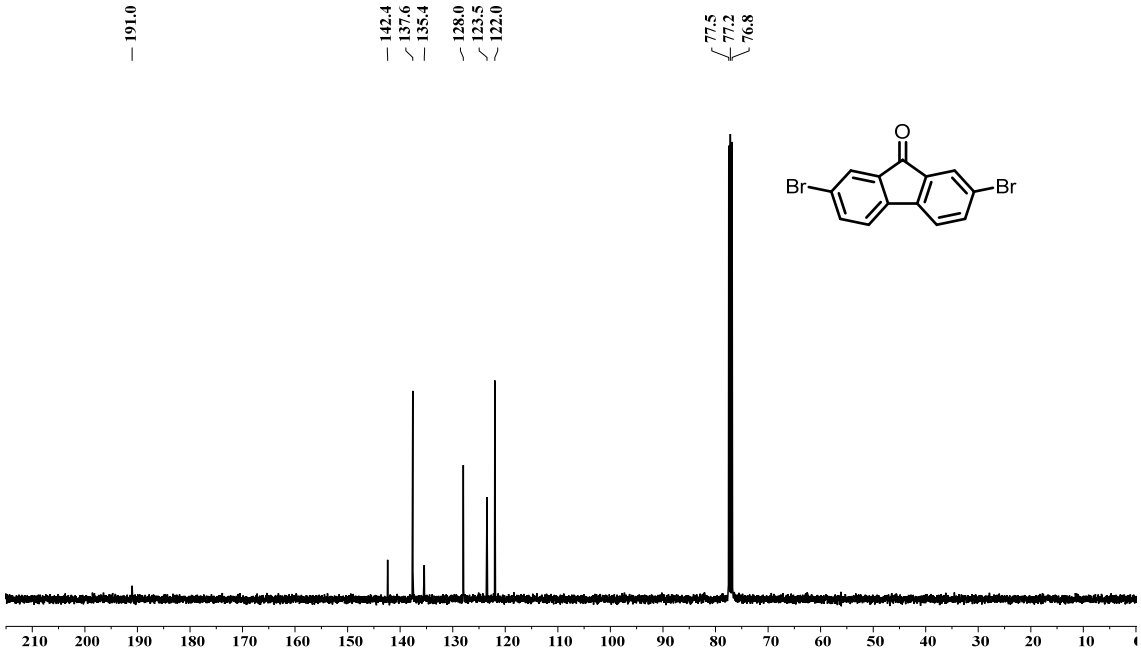

Fig. S56 $^{13}C\{^{1}H\}$ NMR spectrum of **1b** in $CDCl_3$ (101 MHz).

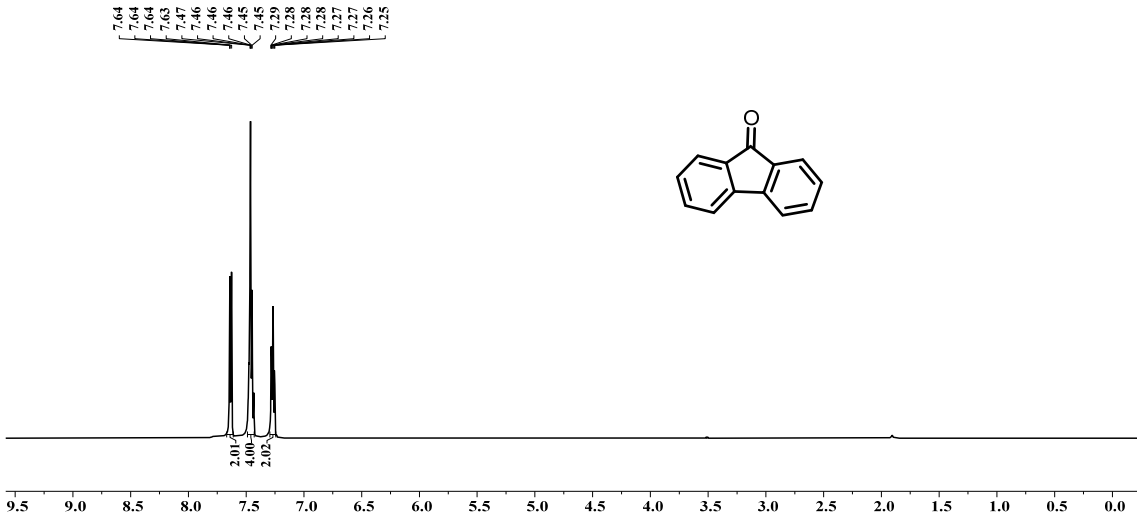

Fig. S57 ^{1}H NMR spectrum of **1c** in $CDCl_3$ (500 MHz).

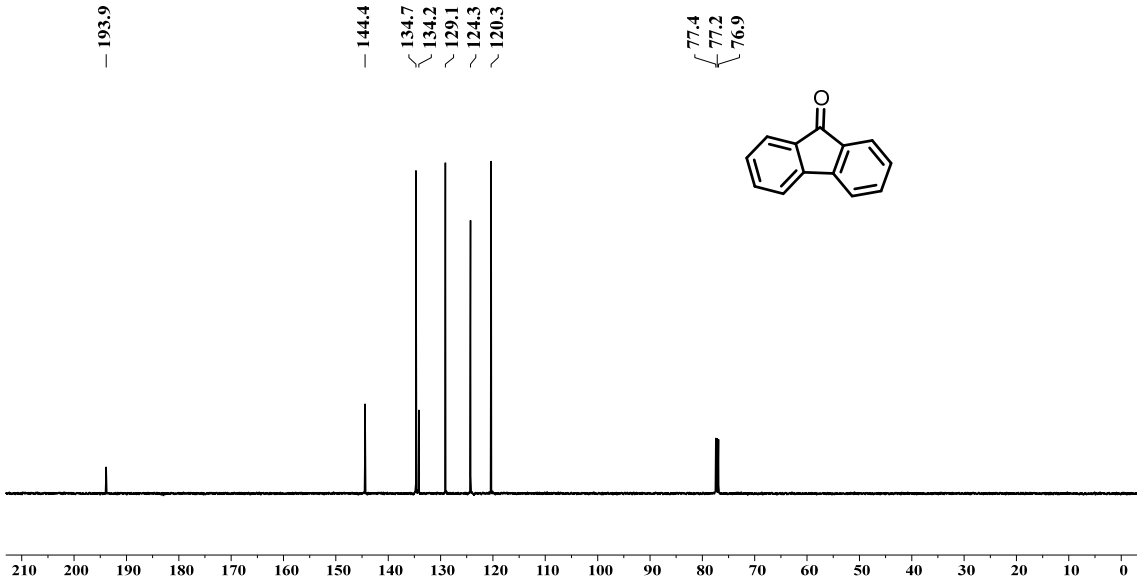

Fig. S58 $^{13}C\{^{1}H\}$ NMR spectrum of **1c** in $CDCl_3$ (126 MHz).

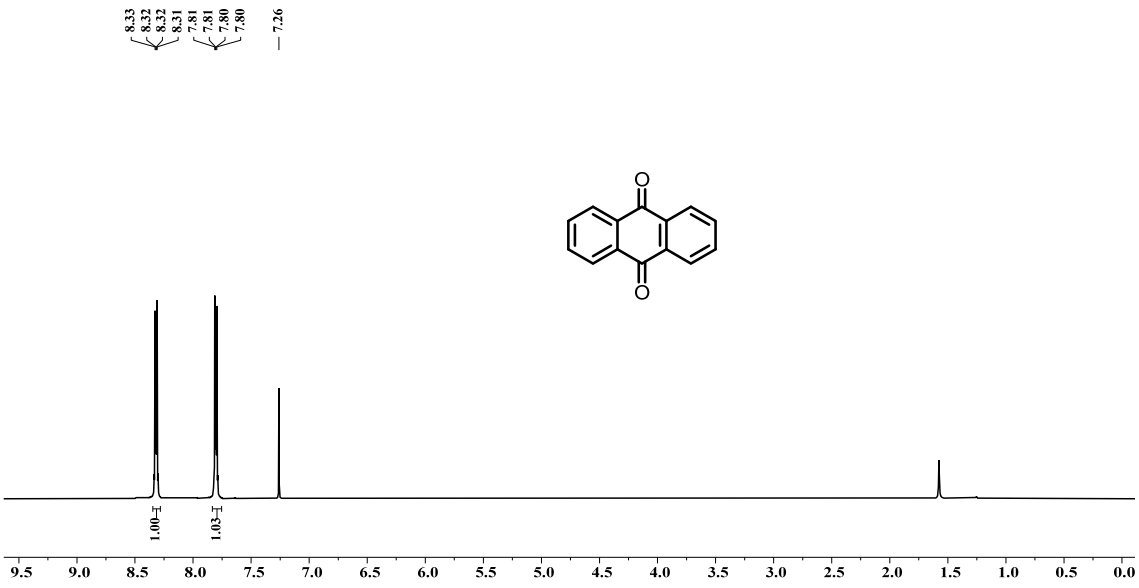

Fig. S59 ^{1}H NMR spectrum of **1d** in $CDCl_3$ (500 MHz).

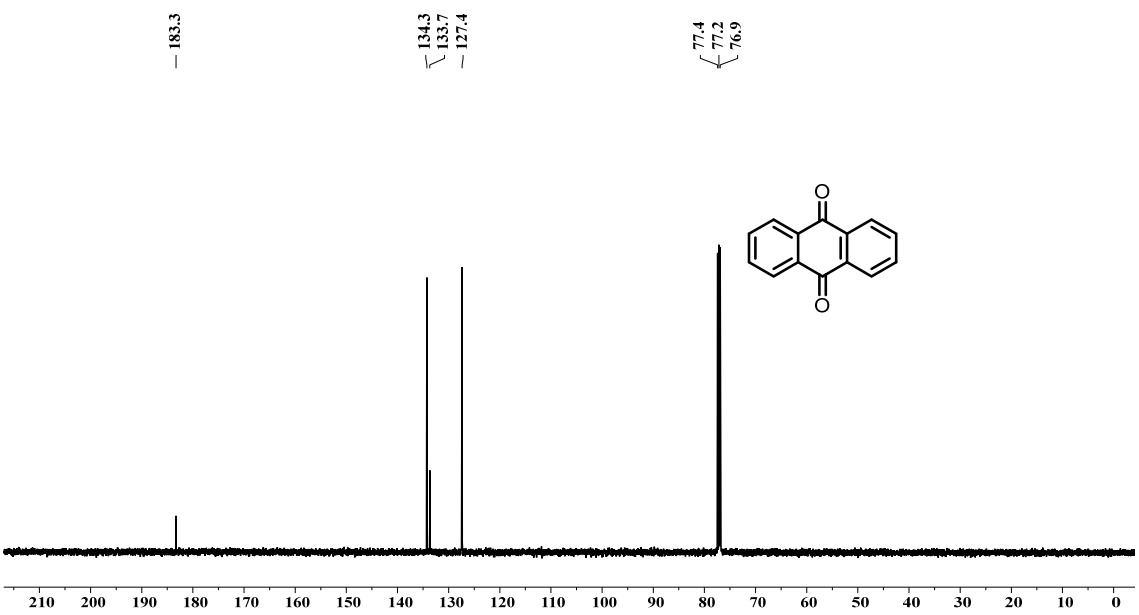

Fig. S60 $^{13}C\{^{1}H\}$ NMR spectrum of **1d** in $CDCl_3$ (126 MHz).

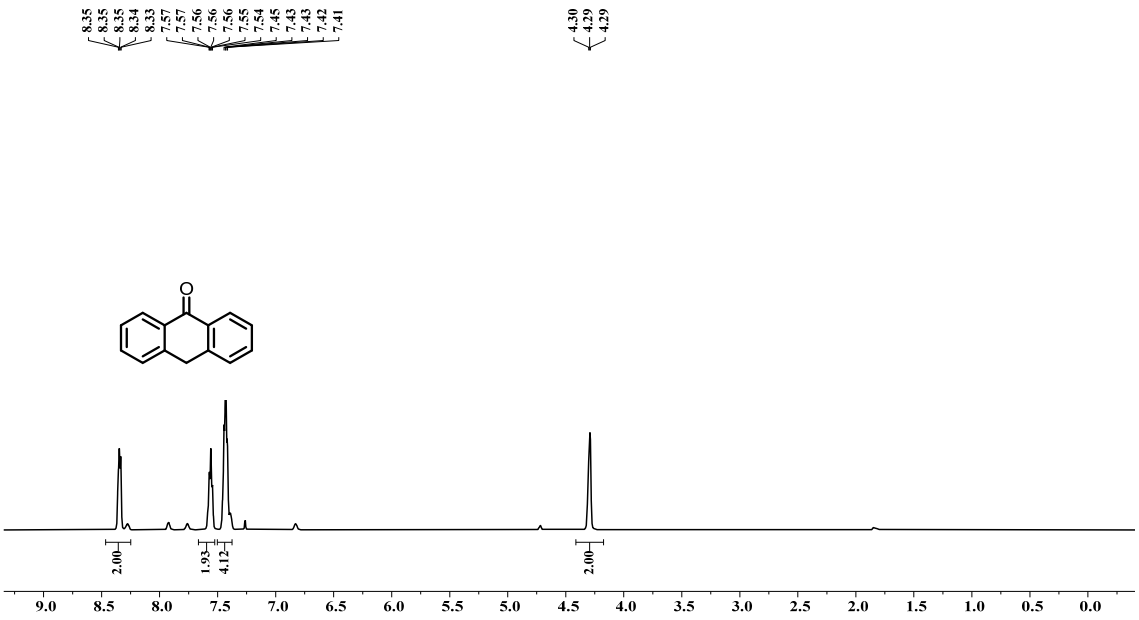

Fig. S61 ^{1}H NMR spectrum of **1e** in $CDCl_3$ (500 MHz).

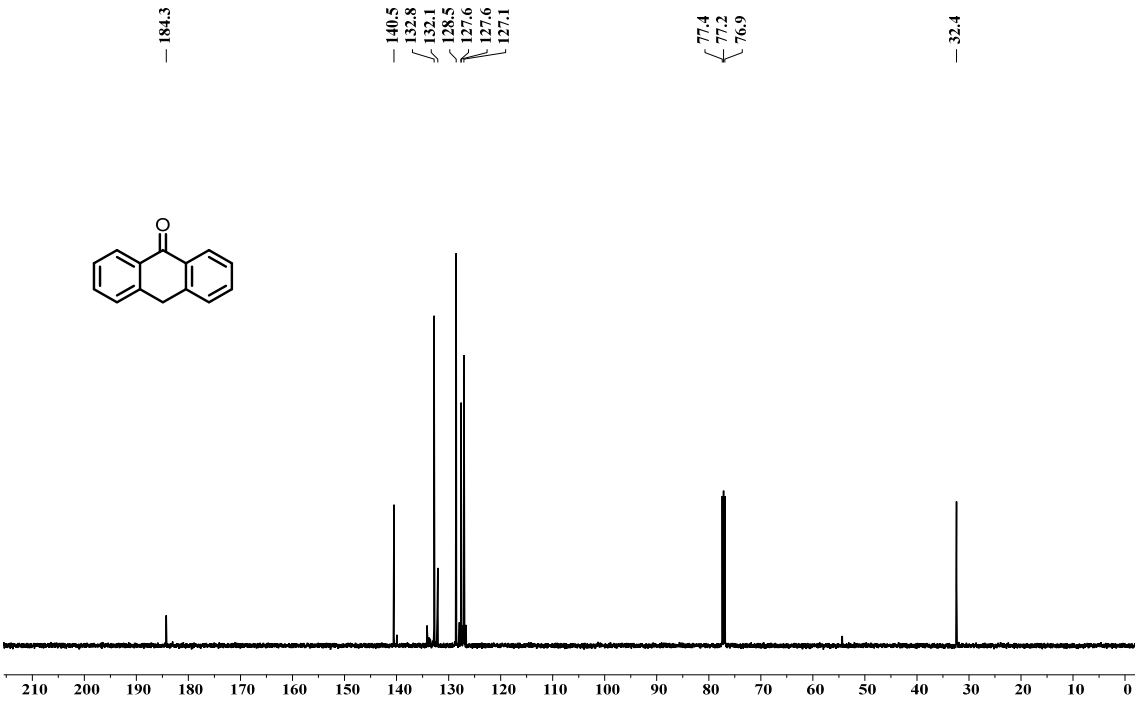

Fig. S62 $^{13}C\{^{1}H\}$ NMR spectrum of **1e** in $CDCl_3$ (126 MHz).

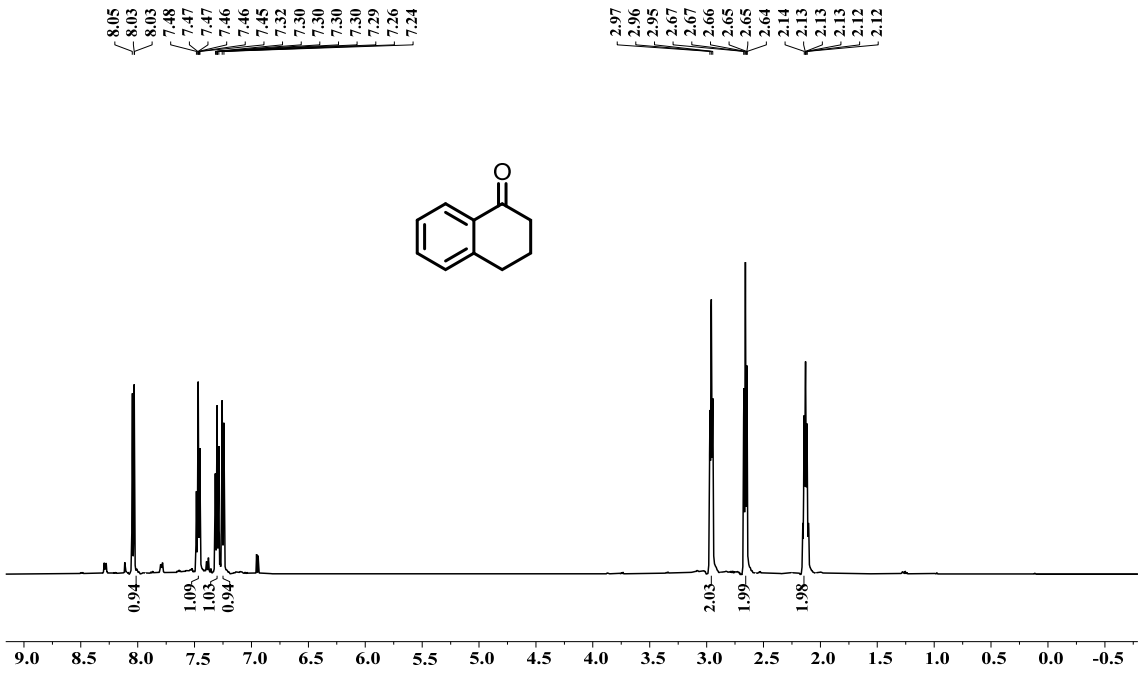

Fig. S63 ^{1}H NMR spectrum of **1f** in $CDCl_3$ (500 MHz).

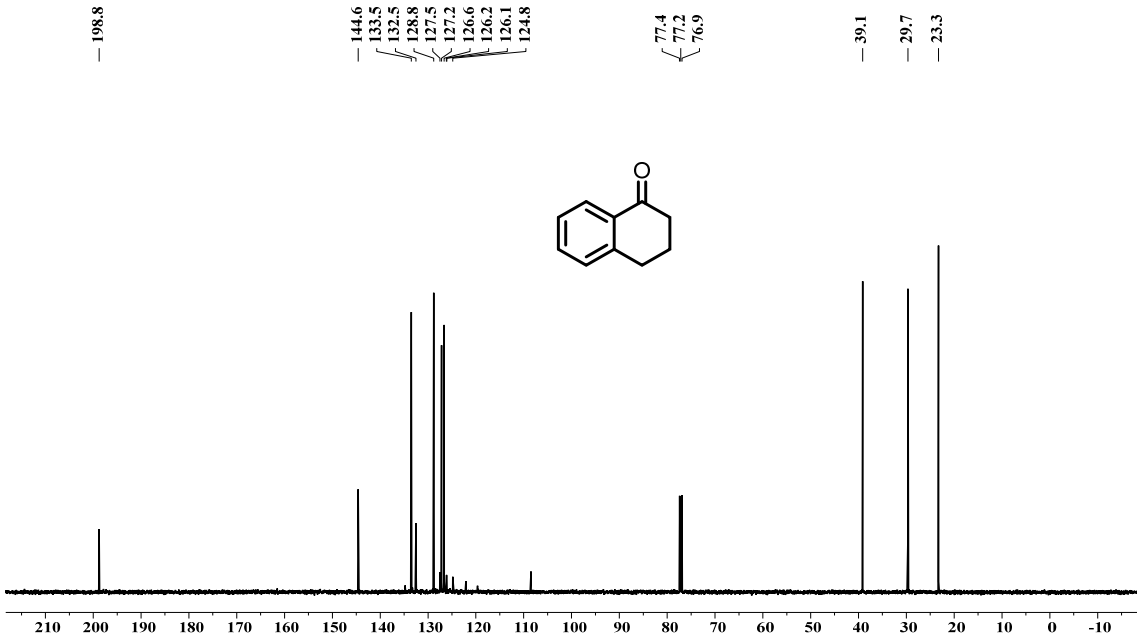

Fig. S64 $^{13}C\{^{1}H\}$ NMR spectrum of **1f** in $CDCl_3$ (126 MHz).

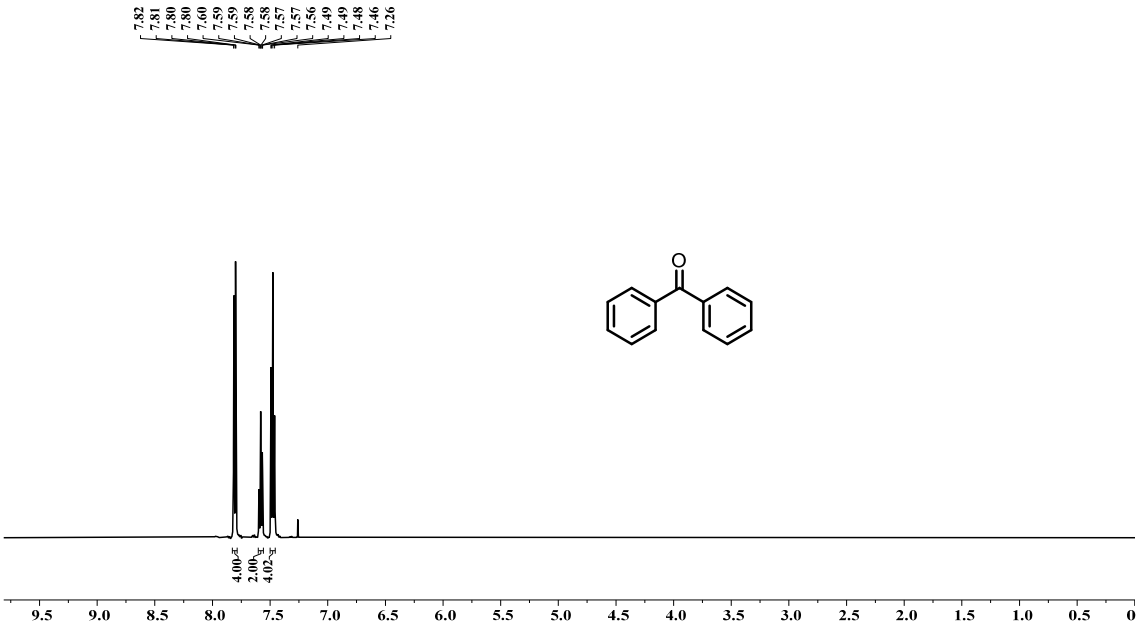

Fig. S65 ^{1}H NMR spectrum of **1g** in $CDCl_3$ (500 MHz).

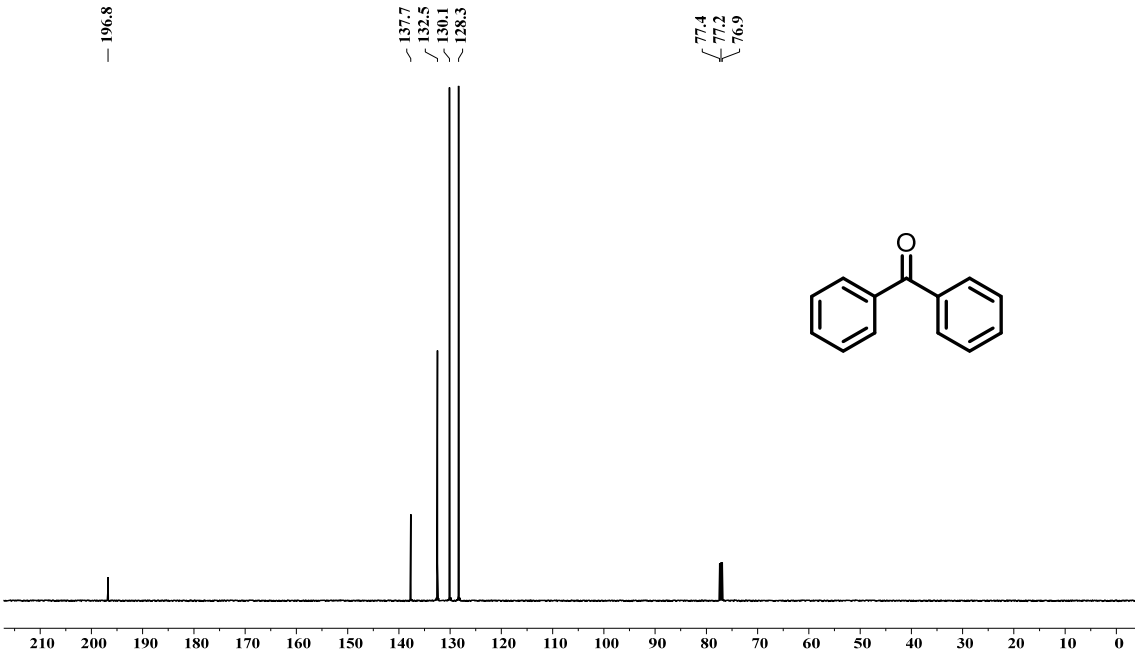

Fig. S66 $^{13}C\{^{1}H\}$ NMR spectrum of **1g** in $CDCl_3$ (126 MHz).

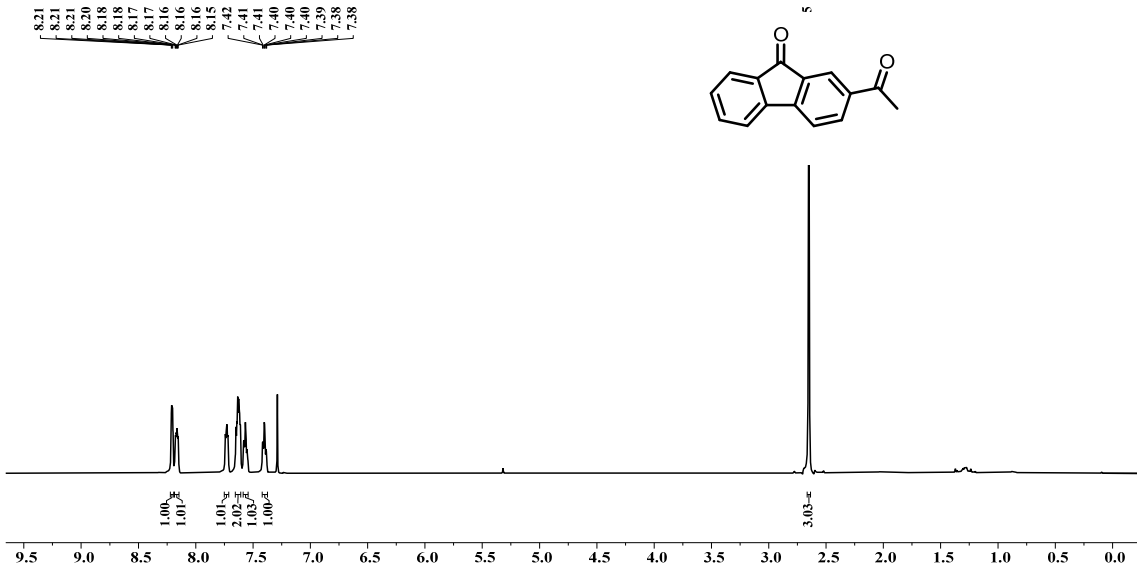

Fig. S67 ^{1}H NMR spectrum of **1i** in $CDCl_3$ (500 MHz).

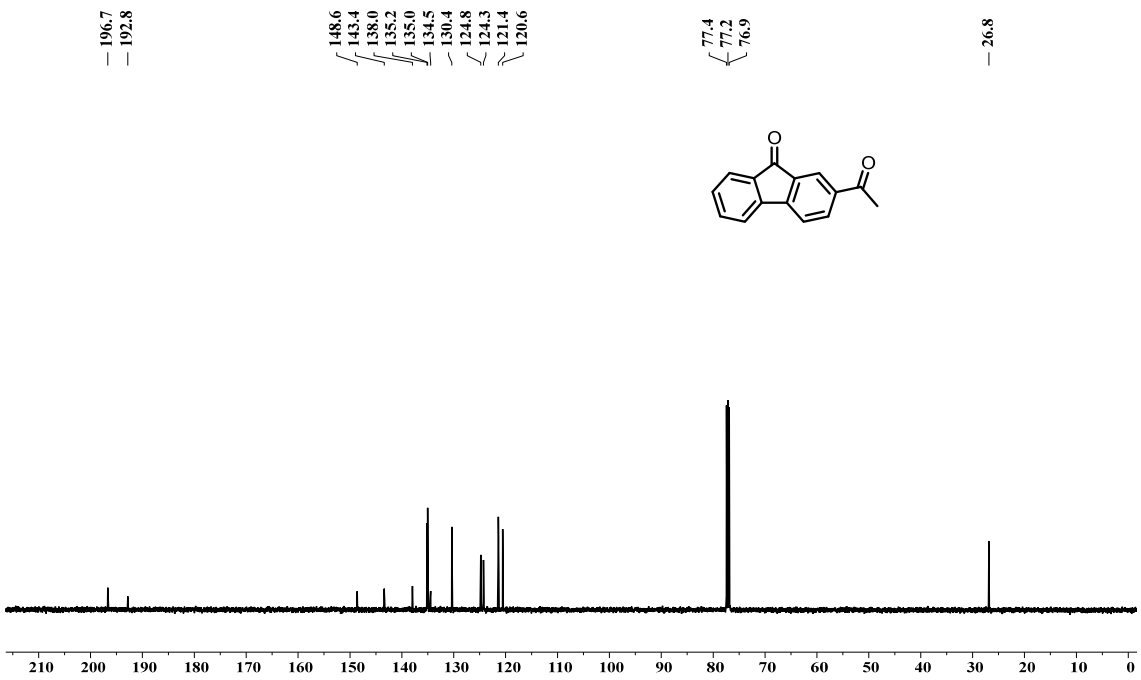

Fig. S68 $^{13}C\{^{1}H\}$ NMR spectrum of **1i** in $CDCl_3$ (126 MHz).

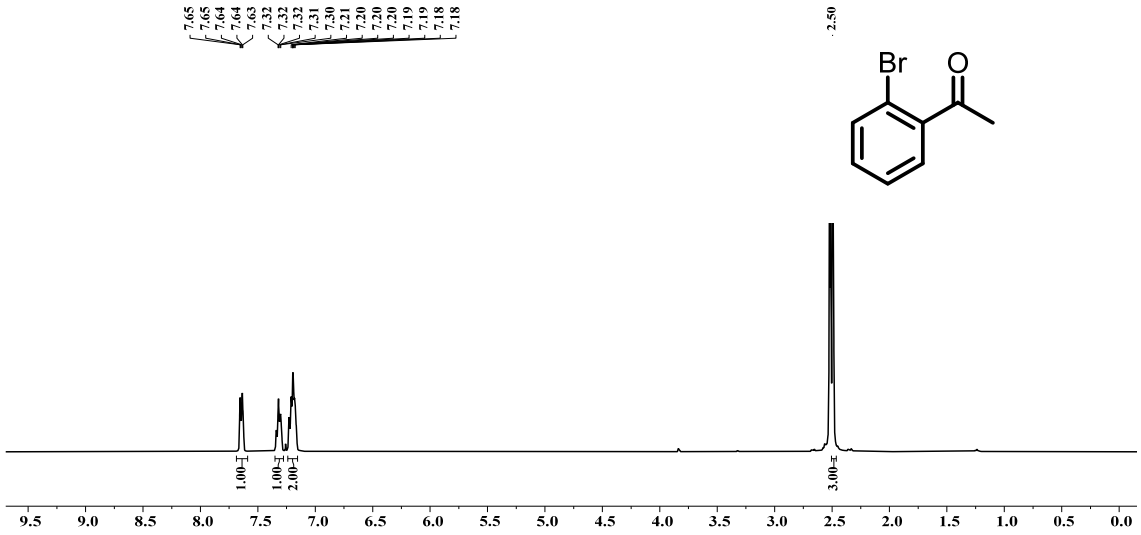

Fig. S69 ^{1}H NMR spectrum of **1l** in $CDCl_3$ (400 MHz).

Fig. S70 $^{13}C\{^{1}H\}$ NMR spectrum of **1l** in $CDCl_3$ (101 MHz).

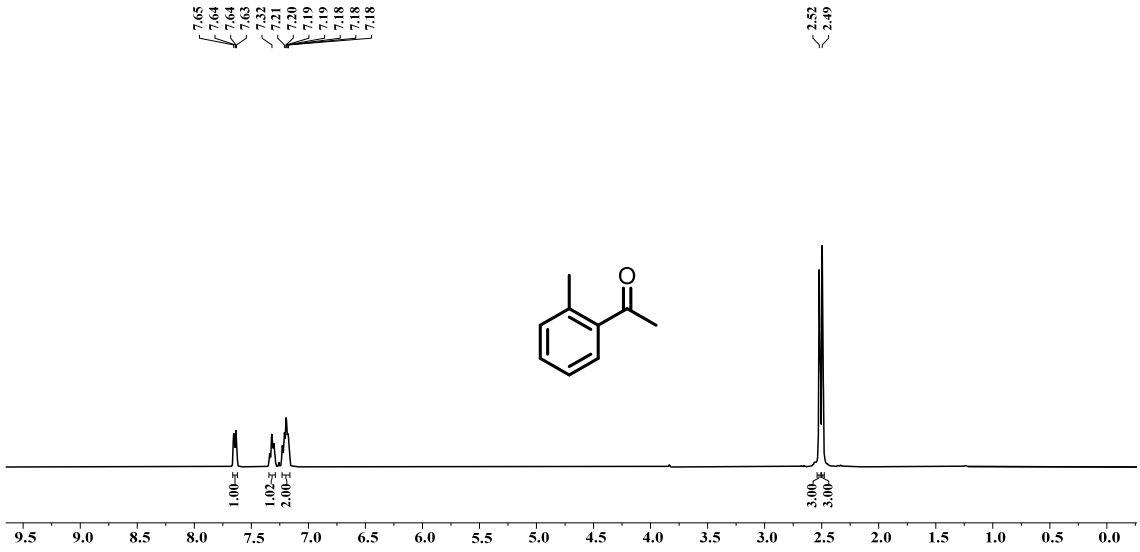

Fig. S71 ^{1}H NMR spectrum of **1m** in $CDCl_3$ (400 MHz).

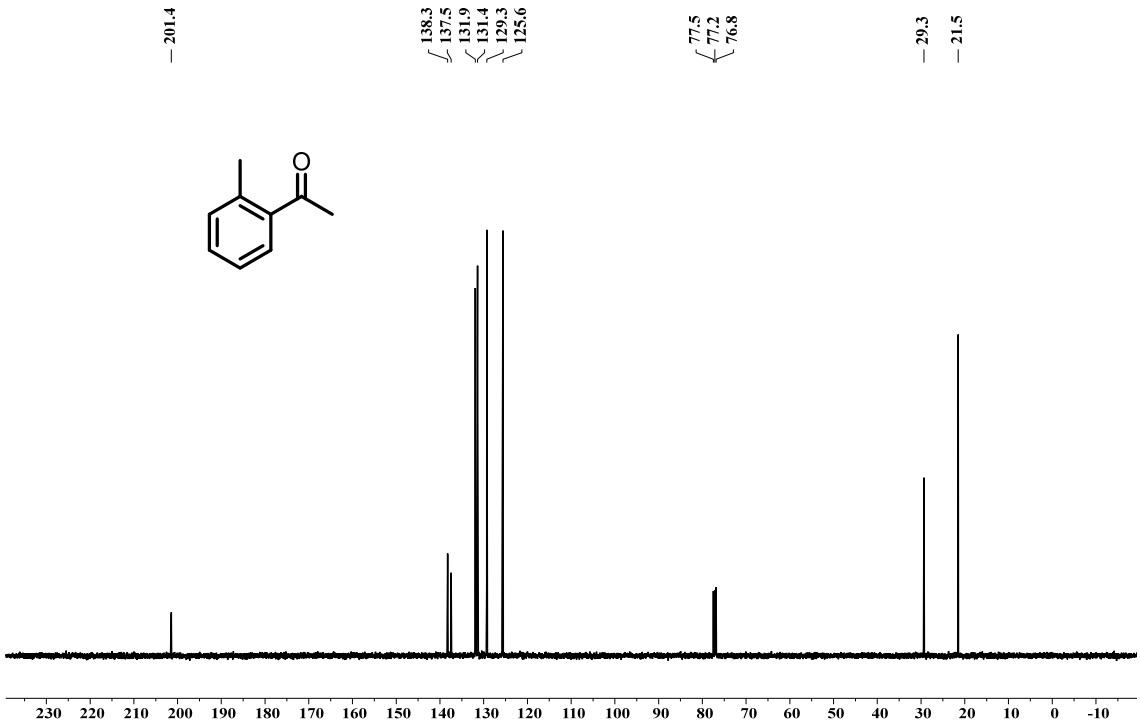

Fig. S72 $^{13}C\{^{1}H\}$ NMR spectrum of **1m** in $CDCl_3$ (101 MHz).

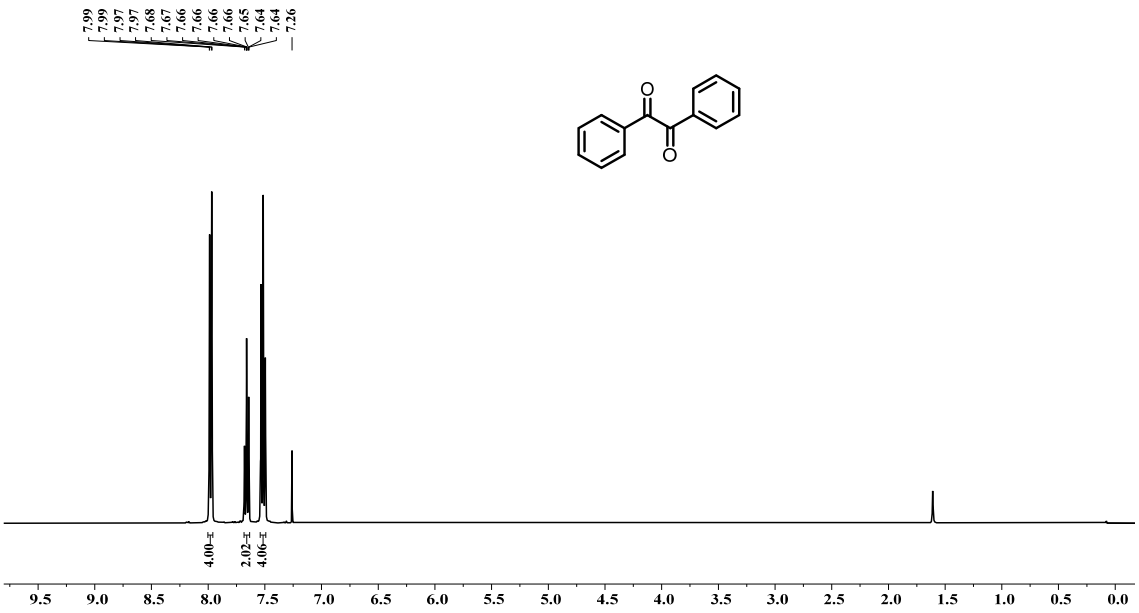

Fig. S73 ^{1}H NMR spectrum of **1n** in $CDCl_3$ (400 MHz).

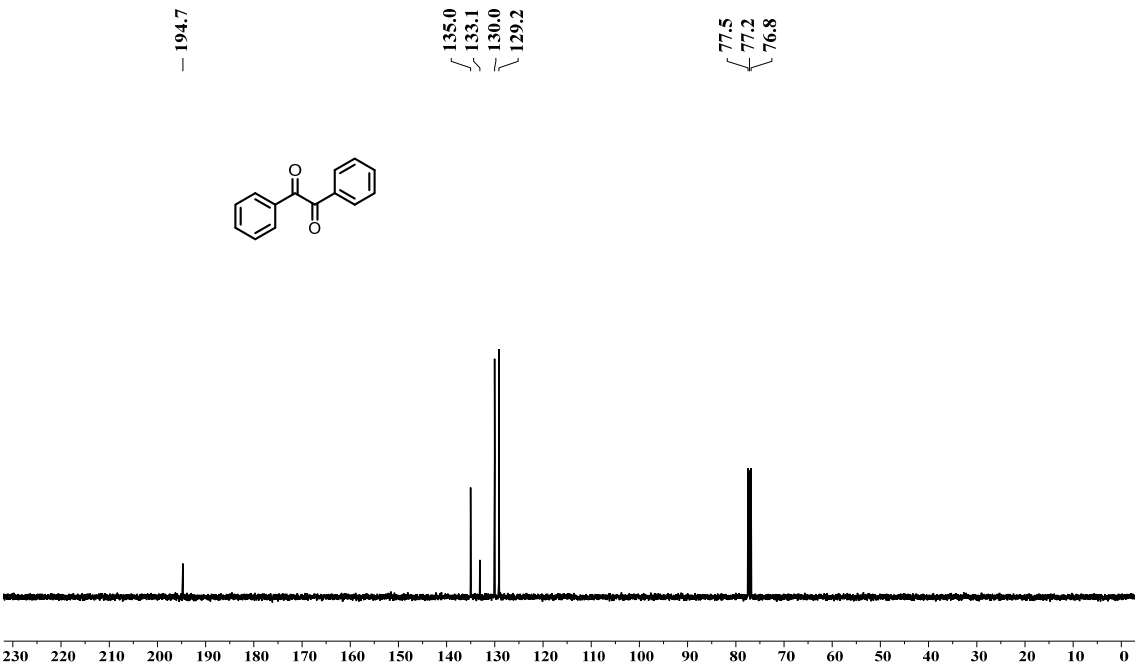

Fig. S74 $^{13}C\{^{1}H\}$ NMR spectrum of **1n** in $CDCl_3$ (101 MHz).

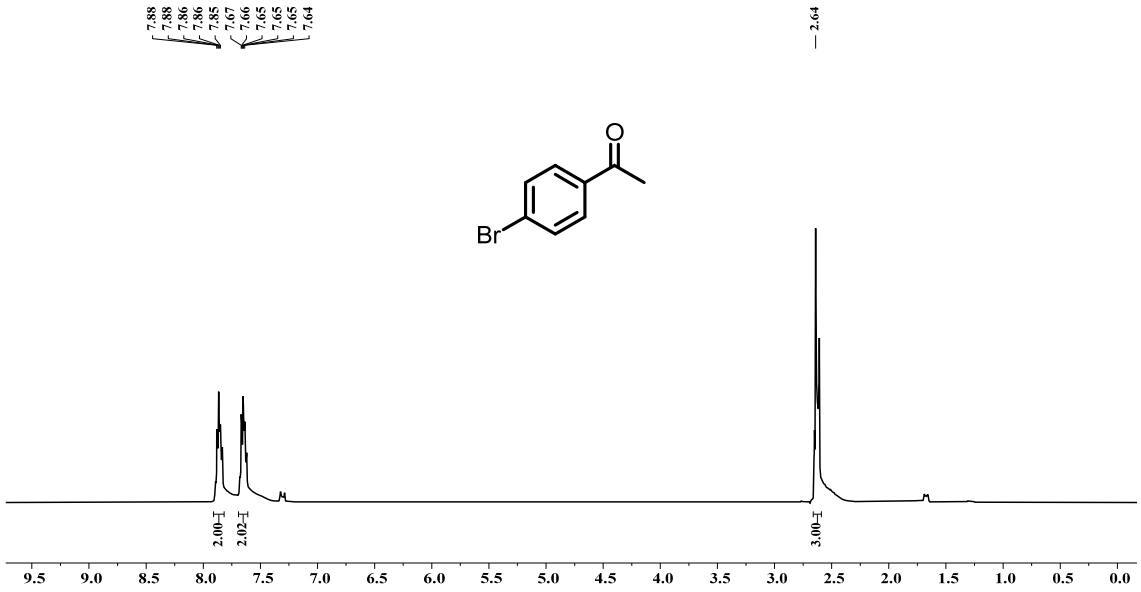

Fig. S75 ^{1}H NMR spectrum of **1o** in $CDCl_3$ (500 MHz).

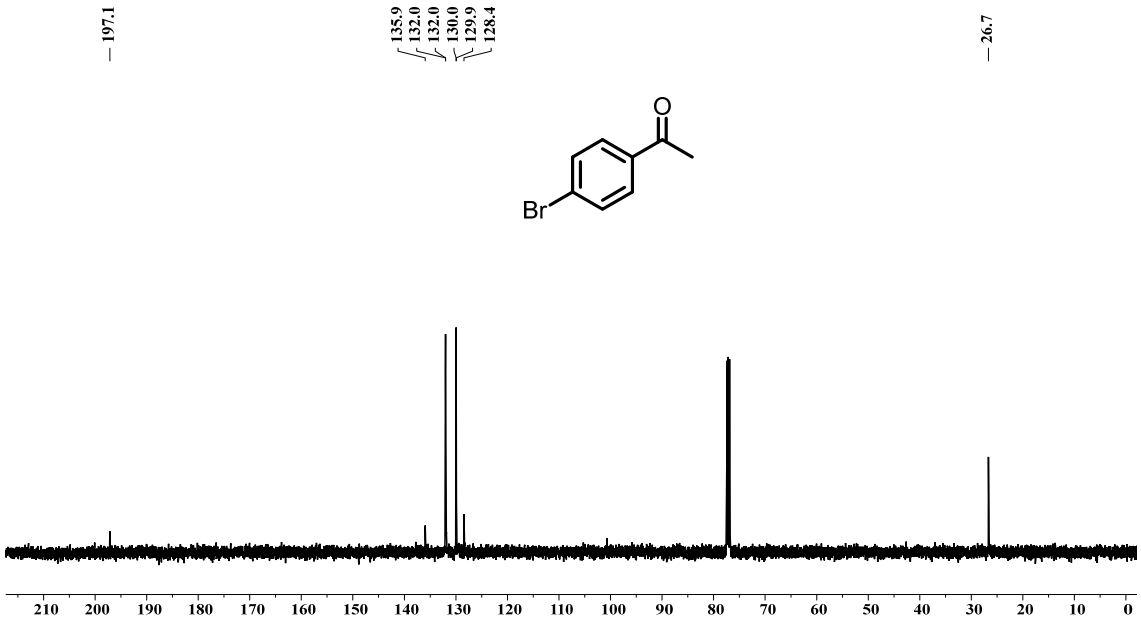

Fig. S76 $^{13}C\{^{1}H\}$ NMR spectrum of **1o** in $CDCl_3$ (126 MHz).

References:

1. J. Jansa, T. Řezníček, L. Dostál, Z. Růžičková, F. Bureš and R. Jambor, *Appl. Organomet. Chem.*, 2016, **30**, 1036-1042.
2. a) G. Ferguson, R. McCrindle, A. J. McAlees and M. Parvez, *Acta Crystal.* , 1982, **B38**, 2679-2681; b) R. A. Baber, A. G. Orpen, P. G. Pringle, M. J. Wilkinson and R. L. Wingad, *Dalton Trans.*, 2005, 659-667.
3. a) D. V. Partyka, J. B. Updegraff Iii, M. Zeller, A. D. Hunter and T. G. Gray, *Dalton Trans.*, 2010, **39**, 5388-5397; b) S. A. Bhat, J. T. Mague and M. S. Balakrishna, *Dalton Trans.*, 2015, **44**, 17696-17703; c) S. Doherty, J. G. Knight, D. O. Perry, N. A. B. Ward, D. M. Bittner, W. McFarlane, C. Wills and M. R. Probert, *Organometallics*, 2016, **35**, 1265-1278.